Dry Metal Forming Open Access Journal

Final Project Report

Edited by Frank Vollertsen
Available online at https://elib.suub.uni-bremen.de

www.drymetalforming.de

Dry Met. Forming OAJ FPR 6 (2020) 069–098
Date of Report 31 March 2020; published 12 June 2020

Dry forming of low alloy steel materials by full forward impact extrusion with self-lubricating tool coatings and structured workpieces

(DFG Grant No. BO 1979/38&44; KL 500/118&141; Funding Period 01.01.2014 – 31.12.2019)

Kirsten Bobzin*[1], Fritz Klocke[2], Thomas Bergs[2], Tobias Brögelmann[1], Andreas Feuerhack[2], Nathan C. Kruppe[1], Rafael Hild[2], Dennis C. Hoffmann[1]

[1]Surface Engineering Institute (IOT), Kackertstr. 15, 52072 Aachen, Germany
[2]Laboratory for Machine Tools and Production Engineering (WZL), Campus Boulevard 30, 52074 Aachen, Germany

Summary

In cold bulk metal forming manufacturing processes high quality components are produced in large quantities. The high process loads lead to wear of the tools, which is reduced by lubricants based on mineral oils and phosphates. As these lubricants are questionable for ecological and economic reasons as well as to human health, their substitution is necessary. However, their absence in the tribological system leads to unknown contact conditions. This research project focuses on dry full forward impact extrusion of steel. The aim of the project is to control the increased process loads, such as contact normal stress, thermal loads and relative speed by a tool-sided and a workpiece-sided approach. The tool-sided approach is the development of self-lubricating coatings, which are deposited by physical vapor deposition (PVD) technology. Taking into account the load collective during dry full forward impact extrusion, the coatings must exhibit high wear resistance and simultaneously friction-reducing properties. For this purpose, coating systems consisting of the wear-resistant hard coating CrAlN were developed, which are modified with tribo-active elements Mo, W and S, which form friction reducing reaction layers MoS_2 or WS_2 under tribological load. The workpiece-sided approach is based on the surface structuring of workpieces by shot peening using various peening parameters and peening media. This allows the adjustment of the real contact surface between tool and workpiece in order to partially exceed the yield limit of the workpiece before volume forming. The influence of self-lubricating tool coatings and structured workpieces on the friction and wear behavior was investigated in a first step by analogy model tests. These findings were then transferred to the full forward impact extrusion process in order to achieve an industrial process under dry tribological boundary conditions. In unlubricated industrial field trials, it was shown for the first time that a dry full forward extrusion process of steel can be achieved by applying self-lubricating tool coatings and the structured surfaces. Analyses of the interaction between the tool coating and the workpiece surface reveal a friction reduction during the first stroke with rougher surfaces, but an increase of the wear compared to smoother surfaces. Additionally, finite element method was used to simulate the dry forming process. Subsequently, a more complex two-shouldered die geometry was considered, which leads to significantly higher tool loads. Based on the field trials, dry full forward impact extrusion of steel was achieved for the first time. Subsequent wear investigations show that coatings have significantly reduced wear.

Keywords: Dry metal forming, self-lubricating coating, structured workpieces, frictional shear stress, PVD

*E-mail address of corresponding author: r.hild@wzl.rwth-aachen.de; hoffmann@iot.rwth-aachen.de

1 Introduction and state of the art

Cold bulk metal forming represents an efficient and resource-saving process for the mass production due to high material utilization of $\Psi_{eff} = 85\ \%$ and high achievable forming degrees up to $\varphi = 0.8$ [1]. These processes are characterized by high product quality, high reproducibility and short cycle times [2]. The full forward impact extrusion is process variant of cold bulk metal forming. According to DIN 8582, full forward impact extrusion is a process which reduces solid material in single and multiple stages under compressive stress [3]. A schematic illustration of the full forward impact extrusion process is shown in Fig. 1 (a). The process begins with a compression of the material by the relative movement of the punch until the yield stress of the workpiece material is reached. The material then flows into the forming die and is reduced. After the reduction shoulder has been overcome, an almost constant force is established, which decreases in relation to the surface contact with the die [2]. After the forming process the workpiece will be removed by an ejector. The punch force depends on the tribological system, the die geometry and the thermo-mechanical properties of the workpiece material [4].

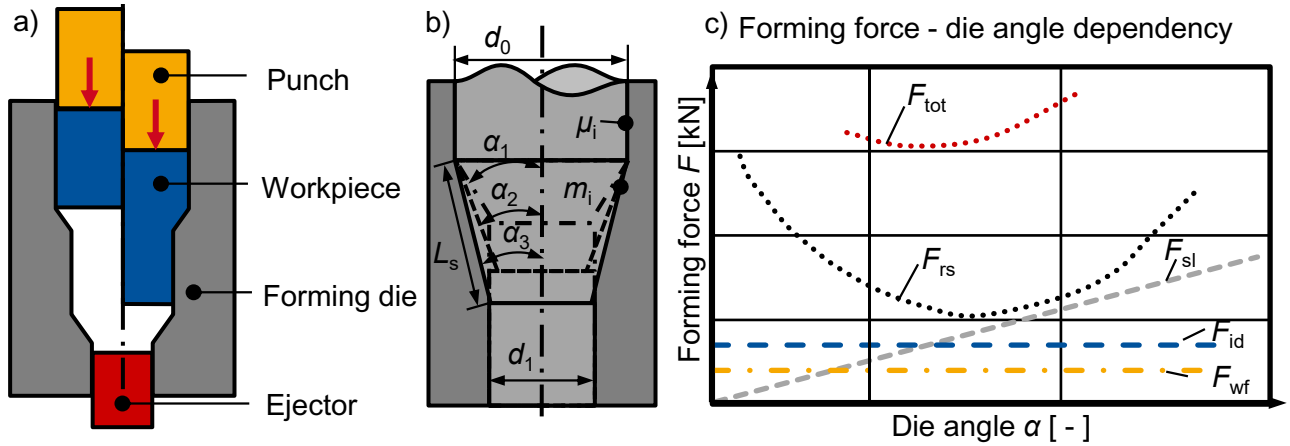

Fig. 1: Representation of the impact extrusion process as well as occurring forces and their magnitude as a function of the die angle [5]

The die geometry is described by the shoulder opening angle α, the input diameter d_0 and the output diameter d_1, Fig. 1 (b). The tool loads depend in turn on the punch force F_p, which corresponds to the total press force F_{tot}. The necessary total force F_{tot} was described according to Doege et al. as follows [5]:

$$F_{tot} = F_{id} + F_{wf} + F_{rs} + F_{sl} \tag{1}$$

The total press force F_{tot} is expressed by the ideal forming force F_{id} required for plastic forming, the force to overcome wall friction F_{WF}, the force to overcome friction at the reduction shoulder F_{rs} and finally the force to overcome internal shear losses F_{sl}, Fig. 1 (c). The specific progression of F_{rs} and F_{sl} as a function of the shoulder opening angle alpha cannot be given in general terms, as these depend, for example, on the length of the reducing shoulder L_S, the degree of forming and the material combination. The ideal forming force F_{id} depends on the workpiece material. The ideal forming force F_{id} cannot be influenced as it depends exclusively on the yield stress of the workpiece material. The friction at the reduction shoulder depends mainly on the internal friction of the material. This is represented by the friction factor law. The proportion is basically dependent on the shear yield limit, which in turn depends on the material. No high plastic deformations occur within the range of wall friction. Therefore, it is possible to model this area with the help of the friction model according to Coulomb. The internal shear losses are basically caused by dissipation [5]. However, conventional friction models, such as the friction model according to Coulomb or the friction factor law, do not adequately depict the influences on the process. The friction model according to Coulomb assumes a proportional relationship between normal force and friction force [6]. However, if the normal forces are too high, the friction force is overestimated and does not reflect real values. The friction factor model, on the other hand, assumes a fixed shear flow limit, above which friction is capped [7]. But friction effects caused by two bodies sliding against each other are neglected. Combinations of both models, such as the friction model according to Tresca [8] or Shaw [9], better represent the real conditions. However, even with these friction models, the influence of distinctive surface conditions of the workpiece or tool is represented in a simplified way using constant values. Bay et al. extended existing friction models. The friction model maps the areas in such a way that the friction model according to Coulomb is valid for low normal contact stress and the friction factor law is valid for high normal contact stress [10]. Another friction model was developed by the

Institute for Forming Technology and Forming Machines from the Leibniz University Hannover. The friction model describes the shear stresses under elastic contact conditions, under plastic contact conditions as well as the influence of relative velocity on friction. Thus, not only the normal contact stress is considered as decisive but also the relative velocity [11]. Another approach was developed for sheet metal forming. Filzek considers friction as a function of contact normal stress, relative velocity and temperature [12]. Based on this, Filzek formulated a friction model, which is adjusted by means of numerical constants that have to be calibrated. To calibrate these numerical constants, experimental investigations, such as strip drawing tests, must be carried out [12].

Due to the high degree of deformation achievable in full forward impact extrusion of steel, the forming tools, in particular the forming dies, are subjected to a comprehensive load collective, for instance, high normal contact stresses of up to $\sigma_N = 2{,}900$ MPa [13], which leads to high tool wear. Therefore, large quantities of various lubricants are currently required to ensure process reliability. In particular, the use of environmentally harmful zinc soaps and zinc phosphating of the workpieces in industrial applications [13]. An analysis of current steps for the application of conversion layers and soaps was carried out, see Fig. 2 [14].

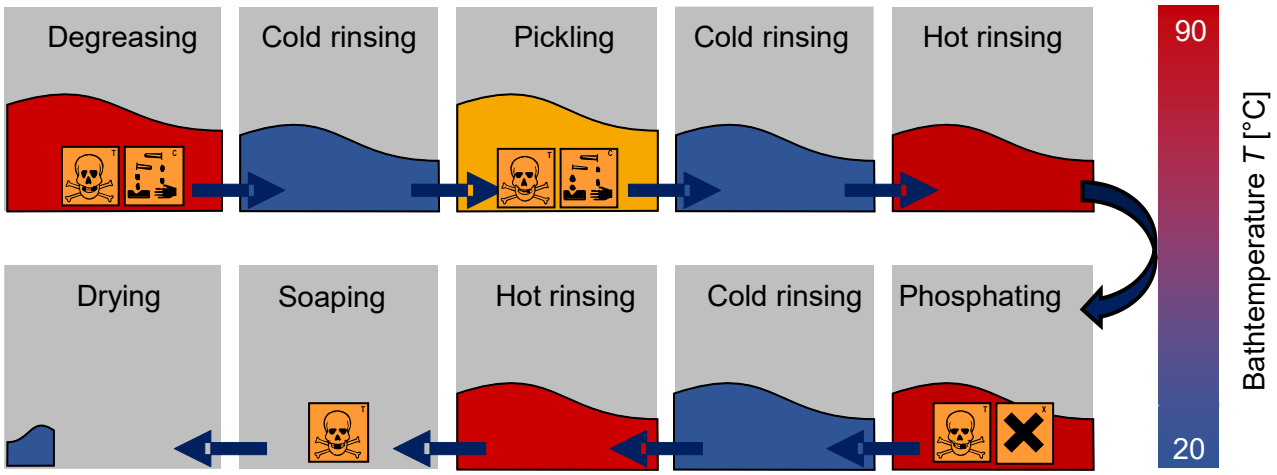

Fig. 2: Process chain for applying a conversion layer and a soap for cold bulk metal forming processes [14]

On the basis of the process chain for the application of the conversion layers and soaps, it can be seen that the process steps of degreasing, pickling, phosphating and soaping are carried out using substances that are harmful to health. In addition, up to ten process steps are generally necessary to apply the phosphate conversion layers in sufficient quantity and thickness so that the workpieces are formed with as little stress as possible, the tools are not damaged and the surface quality of the components is achieved [15]. Furthermore, it must be considered that the formed workpieces have to be cleaned afterwards with considerable effort, which also has a negative influence on the profitability.

However, due to legislative, economic and ecological reasons, there is a huge interest in lubricant-free cold bulk metal forming [16]. Vollertsen and Schmidt redefined dry forming as: “A process where a workpiece leaves a forming tool without the necessity of cleaning or drying before further production steps such as coating or joining processes” [16]. An important basis for changing the process with regard to dry forming is the consideration of the tribological system. According to Czichos and Habig, the tribological system consists of the tool and the workpiece as well as an ambient medium and the intermediate medium [17]. The intermediate medium is not present within the dry forming process which leads to high friction and wear.

Only little research has been carried out in the field of dry forming, and even no research has been carried out in the field of dry cold bulk metal forming of steel so far. Until the implementation of the priority program SPP 1676 “Dry Metal Forming - Sustainable Production through Dry Processing in Metal Forming”, publications in the field of dry forming were limited to the area of sheet metal forming. A solution approach is the application of PVD (physical vapor deposition) coatings, which exhibit good frictional properties in dry tribological contact. Murakawa et al. enabled dry forming in sheet metal forming by means of DLC (diamond-like carbon) coated forming tools [18]. Osakada et al. extended these investigations and analyzed the influence of DLC coatings and their surface roughness on the coefficient of friction during dry boundary conditions [19]. Besides DLC coatings, self-lubricating PVD coatings are also able to reduce friction. Those self-lubricating PVD coatings can be based on transition metal dichalcogenides (TMD) to reduce friction

[20]. Tungsten disulfide (WS_2) [21,22] and molybdenum disulfide (MoS_2) [23–25] are two types of TMD. In such TMD, the crystallographic layers are bonded together with weak van der Waals forces. Thus, leading to a low shear strength and subsequently to low friction [26]. However, self-lubricating coatings, which are based only on TMD, cannot withstand the mechanical loads of full forward impact extrusion of steel due to contact normal stresses of up to $\sigma_N \approx 2{,}900$ MPa [13]. This is attributed to the weak mechanical properties, for example indentation hardness $H_{IT} \leq 8$ GPa [27] and low compound adhesion between the TMD coatings and the substrate [20] compared to hard coatings [28]. For this reason, there is an effort to combine TMD with a wear resistant hard phase to provide resistance to abrasive wear combined with friction reduction. The ternary coating system CrAlN deposited by PVD is a promising candidate for this purpose as it exhibits a high hardness, good abrasive wear resistance and high corrosion resistance [29]. These self-lubricating coating systems can be deposited by various PVD technologies, for example dcMS (direct current Magnetron Sputtering) or HPPMS (High Power Pulsed Magnetron Sputtering). Compared to the HPPMS technology, dcMS is characterized by high deposition rates, which is an important cost factor for industrial coating processes [30]. On the other hand, the HPPMS technology generally operates at short pulse lengths of several tens of microseconds and with frequencies in between of 300 Hz $\leq f_{pulse} \leq$ 4 kHz [31]. Therefore, HPPMS provides higher peak current and higher ionization degree within the plasma compared to conventional dcMS. This leads to higher plasma densities which results in deposition of coatings with dense microstructure and good mechanical properties [32]. Furthermore, HPPMS is advantageous for the deposition of coatings on complex tool geometries, in particular for the coating deposition on geometries with high aspect ratios, for example forming dies. Since the PVD technology is characterized by a strong line of sight characteristic during the deposition process, the HPPMS technology supports coating deposition on complex shaped geometries due to the highly-energetic plasma compared to dcMS [31].The combination of dcMS and HPPMS in a hybrid process combines the advantages of both processes [33].

Earlier efforts such as the Collaborative Research Centre SFB 442 were fundamentally concerned with environmentally compatible tribosystems. Besides the research of novel environmentally compatible lubricants, one focus was to substitute the most harmful lubricants or steps of lubricant application [34]. Various investigations regarding the optimization of the tribological system have shown that a change in the surface structure of the workpiece have an influence on friction and wear [14]. However, the friction models described above do not have the ability to represent the influence of a surface structure of the workpiece or even a coating of the tool. Initial approaches to this were provided by Köhler and Stahlmann [35]. They investigated structured workpieces for the area of solid forming. Stahlmann formulated a friction model based on the surface enlargement and surface modification of the workpieces. Depending on this change, a different amount of lubricant is present in the active joint and thus the friction within the process changes [36]. Hol analyzed in more detail the influence of different roughness peaks on friction. In doing so, he mapped the roughness peaks using a Gaussian distribution and postulated that at the beginning of the process only roughness peaks above the centerline have the possibility to contact the tool and thus influence the friction [37] x. Furthermore, lubricant can only accumulate in the valleys that have the ability to reduce friction [38]. Finally, different attempts were made to model forming processes realistically using different friction models. On the one hand, however, these approaches do not have the potential to represent parameters such as the surface structure of the workpieces or the coating of the tools in addition to the influencing variables of contact normal stress, relative velocity and temperature. On the other hand, some of the models take these parameters into account. Up to now, however, these parameters have only been analyzed under the influence of lubricant on the friction model and therefore do not have the potential to represent a dry forming process.

To meet the objective of the achievement of dry full forward impact extrusion of steel, a tool-sided and a workpiece-sided approach is pursued in this research project within the scope of the SPP 1676. The application of self-lubricating PVD hard coatings on forming dies represents the tool-sided approach to reduce frictional forces between workpieces and tools while at the same time providing wear protection. The workpiece-sided approach provides structuring the workpiece surfaces in order to reduce friction and wear through adapted contact conditions between tool and workpiece. Fig. 3 depicts both approaches to achieving the objective of dry forming. According to the tool-sided approach, the coating system must be designed to adapt to the changing loads along the tool geometry. For example, better friction-reducing properties are required in the inlet area of the forming die than in the area of the reduction shoulders. Since the reduction shoulders are subject to the highest mechanical loads, increased wear resistance is required here compared to the inlet area. The adapted coating properties can be achieved, for example, by adjusting the ratio of the proportion of the wear-resistant ternary hard phase CrAlN and the proportion of the tribo-active elements Mo

and S or W and S. Another approach is to adjust the HPPMS pulse parameters in order to selectively modify the coating properties along the die geometry.

The workpiece-sided solution approach provides texturing the workpiece surfaces in order to reduce friction and wear through adapted contact conditions between tool and workpiece. A distinction is made between stochastic and deterministic surface texturing. The former are achieved by shot peening and the latter by knurling or laser structuring.

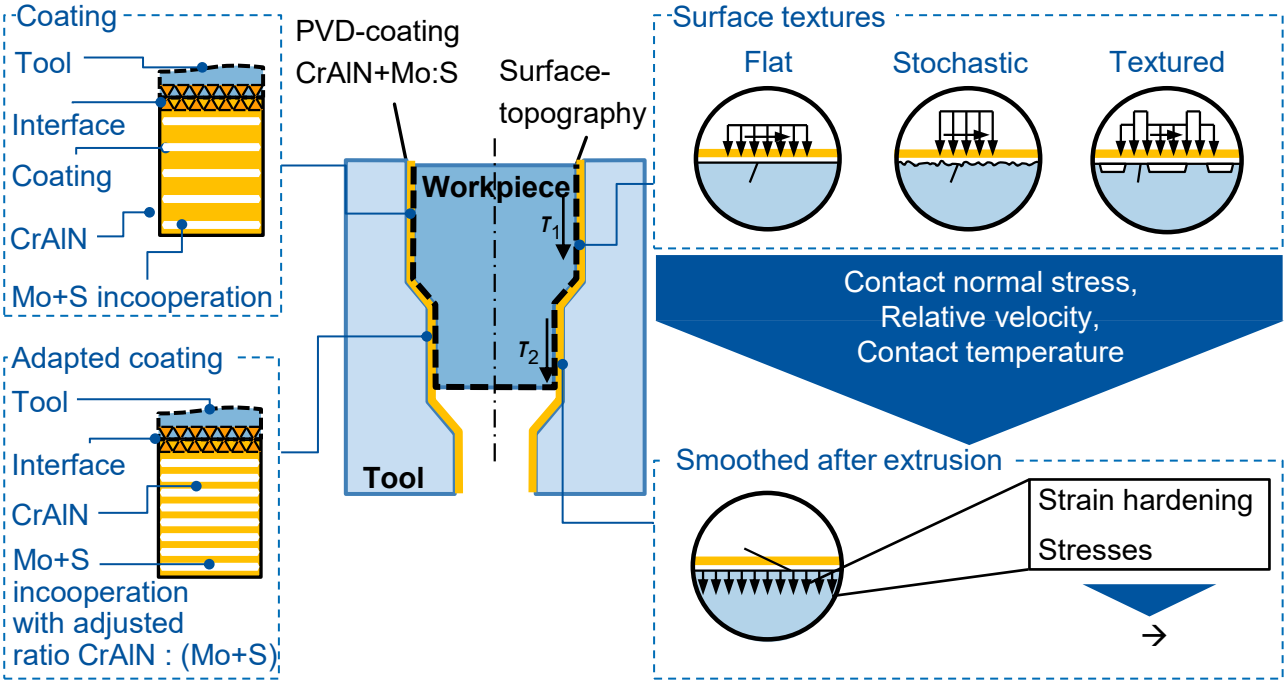

Fig. 3: Schematic representation of the working hypothesis of the research project within the priority program SPP1676

In order to fulfil the objective of realizing a dry full forward impact extrusion process on an industrial scale for the first time, it is necessary to improve the understanding of the complex tribological contact between the self-lubricating PVD coating and the structured workpiece surface. In the tool-sided approach of applying self-lubricating PVD coatings to the forming tools, the first step is to find suitable process parameters for coating deposition in order to synthesize coatings with good frictional properties, high wear resistance and high compound adhesion between coating and substrate. Therefore, the coatings are analyzed in terms of chemical composition, mechanical properties, microstructure, adhesion to the substrate and tribological behavior. With regard to the workpiece-sided approach of structuring workpieces, various surface structures are initially created by means of shot peening and knurling. Parameter studies with different shot peening process parameters and different peening media are performed. Subsequently, the influence of the mechanical workpiece treatment on the resulting properties close to the edge zone, such as roughness and work hardening, was examined. To investigate the interaction between self-lubricating coating and the various surface structures, initially model tests were carried out in an open tribological system. The knowledge obtained was transferred to the real tribological system of full forward impact extrusion and subsequently tested in dry field trials on an industrial scale press with two different geometries of the forming tool.

2 Investigation methods and materials

The case-hardened steel AISI 5115 (16MnCr5, DIN 1.7131) in hot-rolled condition was used as workpiece material, since this is a typical semi-finished product material in cold bulk metal forming [39]. The cold work steel AISI D2 (X155CrMoV12, DIN 1.2379) was used as substrate material for coating deposition. All specimens ($Ø_{Sample}$ = 20 mm, h_{Sample} = 8 mm) were hardened and tempered to a hardness of (61±1) HRC and polished with diamond suspension to an arithmetic mean roughness of $Ra \approx 0.02$ µm. Prior to deposition, the specimens were cleaned in a multi-stage ultrasonic bath, which contained alkaline solvents. Furthermore, an in situ plasma etching process was used to clean the substrates and to ensure sufficient compound adhesion between the coating and the substrate. Such a plasma treatment of the substrate is necessary for the coating to withstand increased tribological tool loads in dry metal forming. The coatings HPPMS CrAlN+Mo:S were deposited in an industrial coating unit CC800/9 HPPMS, CemeCon AG, Wuerselen, Germany and the

coatings hybrid CrAlN+Mo:S were deposited in an modified industrial coating unit CC800/9 CemeCon AG, Wuerselen, Germany. This coating unit was equipped with four dcMS and two HPPMS cathodes.

In order to evaluate the morphology and thickness of the coatings, micrographs of fractured cross sections were taken using secondary electrons (SE) detector in a scanning electron microscope (SEM) ZEISS DSM 982 Gemini, Carl Zeiss AG, Oberkochen, Germany. In addition, analysis using transmission electron microscopy (TEM) regarding the nanostructure was done. A transmission electron microscope (TEM) Tecnai F20, FEI, Oregon, USA, was used which is equipped with Gatan Imaging Filter 2000 (GIF). Drift-corrected EDX-linescan was done in scanning transmission electron microscope (STEM)-HAADF micrograph with a length l = 150 nm and p = 150 measurement points each for an acquisition time t = 10 s. Those investigations have been carried out at the Central Facility for Electron Microscopy (GFE) of the RWTH Aachen University.Measurements of surface roughness were performed according to ISO 25178 by means of a confocal laser scanning microscope (CLSM) Keyence VK-X210, Tokio, Japan. The chemical composition of the coatings was determined using an electron probe microanalyzer (EPMA), Schottky emitter electron microprobe, JEOL JXA8530F, Tokyo, Japan. The analysis were performed with an accelerating voltage of U = 8 kV and a beam current of I = 60 nA. The chemical composition was also determined by using glow discharge optical emission spectroscopy (GDOES). A GDOES profiler type JY 5000 RF, HORIBA Jobin Yvon Ltd., Kyoto, Japan, was used. Optical emission spectroscopy (OES) is used to record the spectra of characteristic wavelengths emitted by atoms in the plasma. By radiation recombination or relaxation, photons are emitted that provide information about the species contained in the plasma. In this work the emission spectrometer EMICON SA, PLASUS GmbH, Mering, Germany was used. A nanoindenter TI 950, Bruker Corporation, Billerica, Massachusetts, USA, with a berkovich indenter was applied for the determination of the mechanical properties indentation hardness H_{IT} and indentation modulus E_{IT}. The constant indentation force used was $F = 10$ mN. The indentation depth was kept below 10 % of the coating thickness. The coatings were examined in as coated condition. Calculations of E_{IT} are based on Oliver and Pharr's equations [40]. A constant Poisson's ratio of $\upsilon = 0.25$ was assumed for the coatings according to previous work. Compound adhesion between coating and substrate was evaluated using Rockwell indentation and scratch test. Rockwell tests were performed and evaluated according to DIN 4856, followed by analyses of residual indents by CLSM. The adhesion strength between substrate and coating can be classified into adhesion classes HF1 to HF6 depending on the damage phenomena at the edge of the Rockwell indent. A quantitative analysis of the compound adhesion between coating and substrate was achieved by scratch testing according to ISO 20502 (DIN EN 1071-3). In this regard, the scratches were performed at different loads and the adhesion between substrate and coating was quantified by CLSM through determination of the critical scratch loads L_{C1} - L_{C3}. The critical scratch loads L_{C1} - L_{C3} were determined depending on the extent of the damage phenomena in and at the edge of the scratch track. The higher the critical scratch loads, the better the compound adhesion between coating and substrate.

Additionally, tribological tests were performed in a Pin-on-Disc (PoD) tribometer, Anton Paar, Peseux, Switzerland, (former CSM instruments SA). Pins of hot rolled AISI 5115 with a radius of $r_{pin,PoD} = 6$ mm and a hardness of $H = 200$ HV0.5 were chosen as counterparts. Pins were pressed in off-center position onto the uncoated reference specimen and the coated samples, Fig. 4 (a). A constant normal force of $F_N = 10$ N was chosen for the PoD tests.

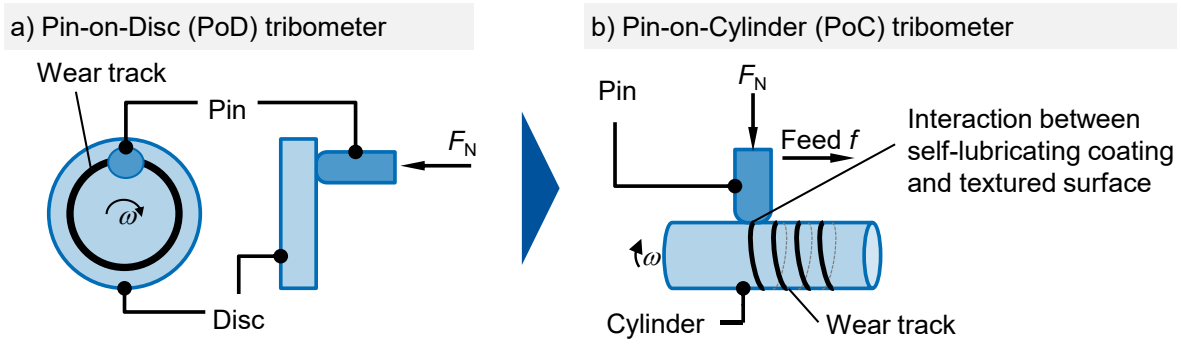

Fig. 4: Schematic illustrations of the operating principle of a pin-on-disc tribometer (a) and the pin-on-cylinder tribometer (b)

The subsequent wear analyses were carried out using CLSM. In order to determine the influence of surface structure on friction, it is necessary to generate comparable loads for cold bulk metal forming and particularly for full forward impact extrusion. Furthermore, it is necessary to analyze the surface structure. The use of

a conventional PoD tribometer would not make this possible. On the one hand only low loads could be applied with the PoD, on the other hand the same friction path is chosen for each revolution. Therefore, a PoC tribometer was developed by the Laboratory for Machine Tools and Production Engineering (WZL) of the RWTH Aachen University und used to investigate the interaction between self-lubricating PVD coatings and various surface structures within tribological contact. By coupling the rotation of the cylinder which represents the workpiece of AISI 5115 to be formed and the feed of the pin which represents the coated forming tool of AISI D2, an open tribosystem is created. In the tribological system of the PoC, the pin with a radius of r = 25 mm is continuously in contact with a surface structure in its initial state. With the help of a hydraulic power unit, it was possible to apply normal forces of up to F_N = 2,600 N, Fig 4 (b). Based on the contact surface, contact normal stresses in the range between p = 500 MPa and p = 1,500 MPa are possible. In further tests the temperature was also varied between T = 20 °C and T = 250°C in order to determine the influence of the temperature on the friction and on the wear of the self-lubricating tool coating.

In order to analyze the influence of the tool geometry, whether one reduction shoulder or two reduction shoulders are present, these geometries were selected, Fig. 5. Furthermore, the load collective on the forming tool is changed.

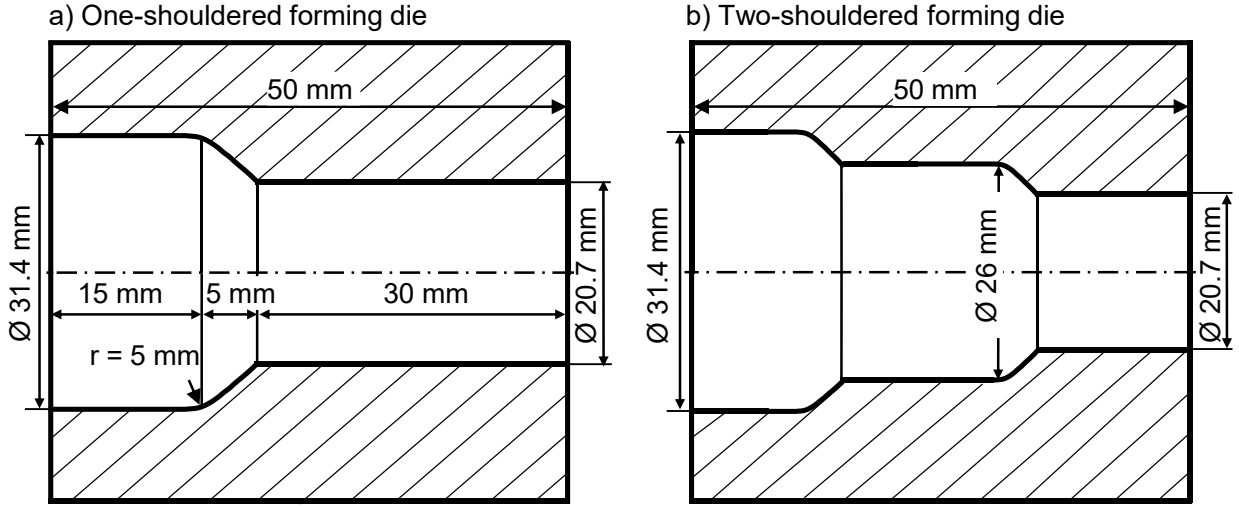

Fig. 5: Schematic illustrations of the one-shouldered (a) and two-shouldered (b) die geometries tested in industrial field trials

First, the one-shouldered dies are investigated in dry industrial field trials. Subsequently, it is required to transfer the previously obtained findings to dry forming by means of two reduction shoulders, since the load collective present on the two-shouldered die is significantly increased. All investigated forming dies consist of hardened cold work steel AISI D2.

3 Development and analysis of workpiece surface structures

The properties of a surface are characterized by its surface integrity. Surface integrity is composed of roughness, hardness, residual stress, chemical composition and other aspects. For this reason, different surface structures are generated and analyzed at the beginning. Then individual surface structures are selected and kept constant for further investigations. In order to analyze the effects of the surface structures on friction and wear in a simplified way, analogy tests are carried out. However, since different loads are present in the individual areas within the impact extrusion process, it is necessary to use different analogy processes. Comparatively low contact normal stresses, temperatures and relative speeds are present in the shaft area of the die. For this reason, it is possible to model the friction conditions with the help of the friction model according to Coulomb. Therefore a PoC tribometer is used. For the area of the reduction shoulder, where much higher contact normal stresses, temperatures and slightly higher relative speeds prevail, it is necessary that the workpieces are exposed to greater plastic deformation. This range is usually represented by the friction factor law, as this sets the shear flow limit as the upper limit for the frictional shear stresses that occur. An established test for determining the friction under these loads is the ring compression test. Therefore, the surface structures are examined with this test.

At the beginning different surface structures were created, analyzed and published in [41]. In order to achieve the greatest possible variation in properties, the surface parameters and surface media listed in Tab. 1 were used.

Tab. 1: Processing parameters of the shot peening process depending on the peening media used and resulting surface properties

Peening media	Peening parameters		Surface properties		
	Pressure p [MPa]	Coverage c [%]	Hardness H [HV10]	Mean arithmetic height Sa [µm]	Maximum height Sz [µm]
Reference			355	0.17	3.53
Corundum	0.4	100	600	3.42	43.20
Ceramic-mix	0.2	100	370	0.81	14.70
Steel	0.3	100	400	1.75	19.40

The resulting surface properties vary considerably from one another. The reference structure is a turned and ground surface. The reference surface exhibits no hardening and a low surface roughness. The surface is hardened and roughened by shot peening the surface. This is most obvious when using corundum particles with high peening pressure. Corundum particles have a shrapnel shape and are therefore very sharp-edged. Furthermore, the particles themselves exhibit high hardness. In comparison, ceramic-mix and steel balls lead to a lower surface roughness and a lower hardening due to the peening pressure used and on the other hand to the lower hardness. The visual appearance of the samples also varies considerably both before and after the tribometer examination, Fig. 6. The reference surface is the smoothest surface. The samples treated with ceramics or steel show a clear change, whereby the surface shows that balls were used as peening medium, since individual craters are still detectable.

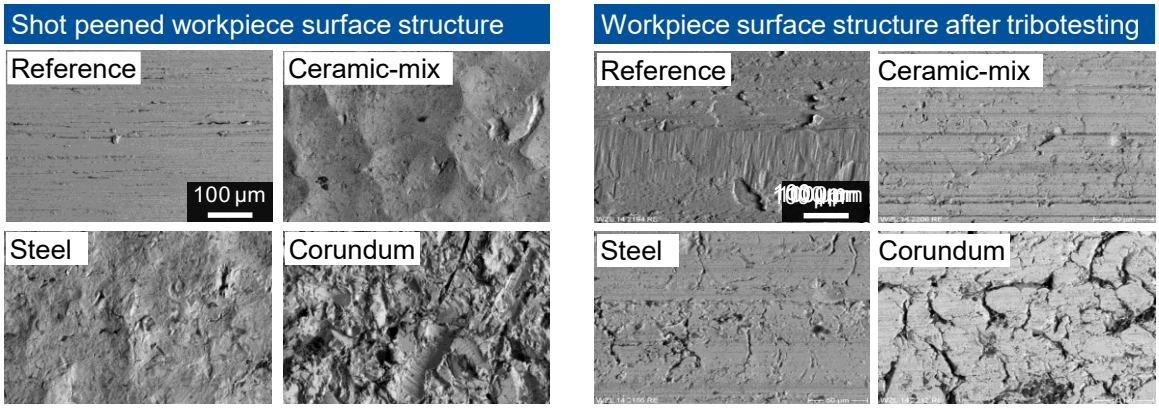

Fig. 6: SEM images of the generated surface structures of workpieces of AISI 5115 before and after the tribometer test

The surface peened with corundum has the roughest surface. After processing, comparable surfaces show up. Only the surface peened with corundum shows clear notches even after the tribometer tests.

3.1 Effect of the workpiece surface structure on leveling and friction

As initially described, the surface integrity of the individual surface structures was analyzed. However, this only provides information about individual properties of the structure. In order to determine the totality of the properties and to get an insight into the mechanisms of action between surface integrity and friction and wear it is necessary to perform other analyses. For this purpose levelling tests were carried out, Fig. 7. Levelling tests have the potential to determine the surface structure as a function of its initial hardness and roughness and then to explain the mechanism of levelling as a function of the contact normal stress up to the approximation of each structure to each other. In order to determine the effect, the individual surfaces were loaded by a spherical basic body with a radius of $r = 5$ mm. Depending on the initial roughness and hardness, the levelling of the surface structure took place as a function of the applied normal force. This levelling can be described with the following formula. The roughness Sa is the potential for levelling and the hardness HB of the surface is the resistance to levelling. Finally, the contact normal stress is related to the normal force and causes the levelling of the roughness peaks. The height t is used to describe the levelling that has taken place so far. A rough and hard surface thus has a higher levelling value than a smooth and soft surface. If the levelling of the roughness peaks and thus the surface structure is complete, then all structures will equalize. This is due to the fact that, on the one hand, the roughness is only in the edge zone and, on the other hand, only the edge zone has been work hardened. In case of complete levelling, each surface has the same roughness and the hardness of the base material, as the work hardening of the workpiece material after shot peening is only present in the edge zone up to a depth of approx. $d = 300$ µm.

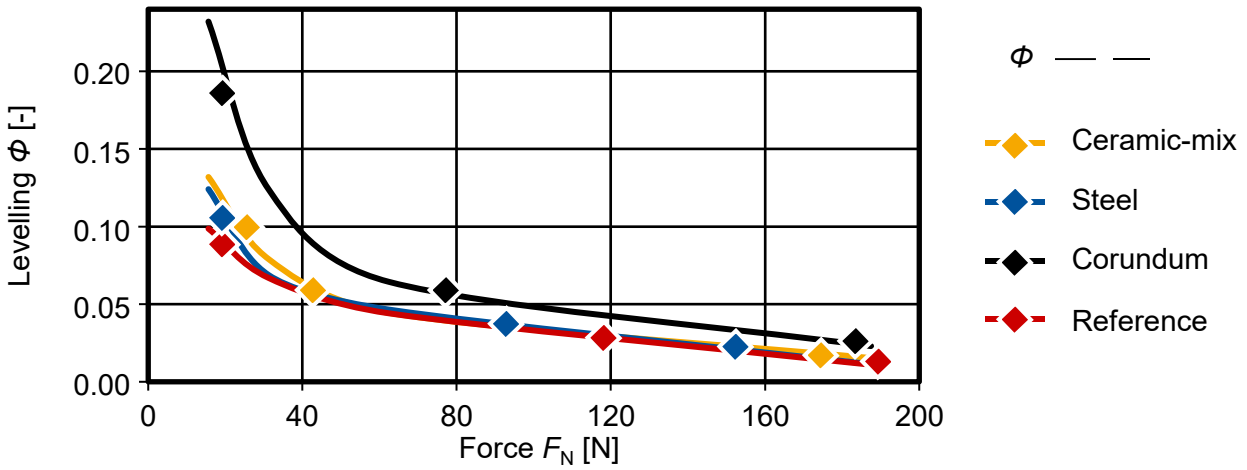

Fig. 7: Determination of a levelling factor as a function of the normal force of the different surface structures of the workpieces of AISI 5115

In order to analyze the effects of the surface structuring on the frictional behavior, PoC tests were conducted with two different normal forces of $F_N = 640$ kN and $F_N = 2{,}600$ kN, see Fig. 8. The results show a clear variance as a function of the contact normal stress.

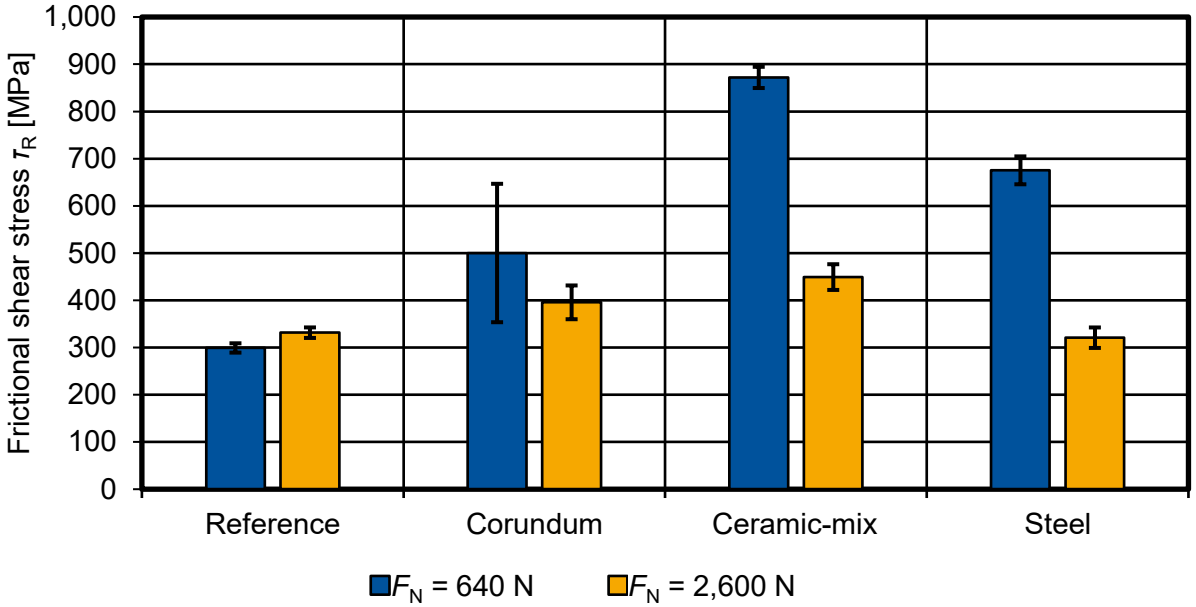

Fig. 8: Influence of the surface structures of workpieces consisting of AISI 5115 on the frictional shear stress in the pin-on-cylinder test as a function of F_N with counterpart pins consisting of AISI D2

At low normal forces, a view of the contact with an uncoated pin shows that a smooth and soft surface, like the reference, achieves the lowest frictional shear stresses. The next highest frictional shear stresses, however, were achieved with the roughest and hardest surface structure. In contrast, surface structures of hardness and roughness in the middle, produced by ceramics and steel, led to the highest frictional shear stresses. Using higher normal forces, the surface structures become similar. Here again, the relationship between levelling and normal force can be seen. With increasing normal force, the levelling is faster and the differences between the individual surface structures become smaller. A semi-finished product peened with steel shows the lowest frictional shear stresses. Slightly higher frictional shear stresses are found on the reference surface. The highest frictional shear stresses were again produced using a surface structure created by ceramic balls. There is no tendency towards an optimal structure with regard to the reduction of frictional shear stresses. Depending on the loads, clear differences can be seen. These differences can also be expected in the course of full forward impact extrusion depending on the tool area. In order to cover the load range of the reduction shoulder, ring compression tests were carried out, Fig. 9. For these tests a numerical FE process simulation is set up at the beginning. Within this simulation the material model of the respective material is used. Furthermore, the friction factor m is varied in the simulation in the range of 0 - 0.57 [42]. This the physically reasonable cover of the friction factor range. The resulting curves are plotted in a diagram as a function of height h and the inner diameter d_i of the ring samples. The resulting diagram serves as the basis

for the experimental procedure. The ring samples are compressed step by step between two upsetting tools. Equidistant steps of 0.4 mm are maintained. After each of these steps the height and diameter of the ring samples are measured. The resulting measured values are entered into the numerically determined diagram.

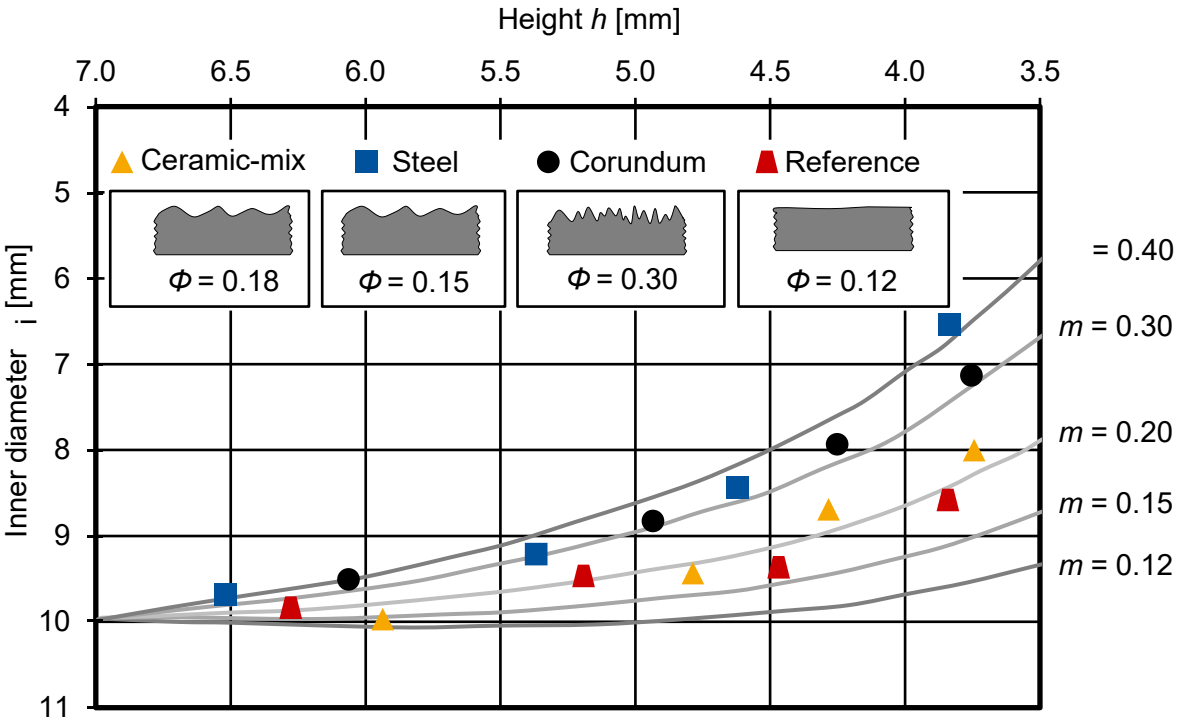

Fig. 9: Determination of friction factors *m* using the ring compression test, taking into account the influence of the surface structure of the workpieces consisting of AISI 5115 on friction [42]

Thus the corresponding friction factors *m* are obtained. The measuring points of the different surface structures can be seen. It can be seen that the surface structure also has an influence on the friction in the area of large plastic deformation. All friction factor *m* lie in a range from 0.2 to 0.4. The highest friction factor is $m = 0.4$ for the surface peened with steel balls. The next lowest coefficient of friction is 0.3 for the surface peened with corundum. The surface peened with ceramics and the reference surface are similar and lie in the range of 0.2. This shows partly contrary tendencies to the tribometer test. While in the tribometer test the ceramic peened surface showed the highest frictional shear stresses, this surface showed the lowest friction factor in the ring compression test. With the help of the investigations of the various workpiece structures it was possible to explain the influence on the friction under low loads as in the shaft area during full forward impact extrusion and under high loads as in the reduction area during impact extrusion. The surface structure has an influence on the friction especially in the running-in area. The structure offers a potential for levelling. This potential for levelling makes it possible to reduce friction, since there are only a few roughness peaks in contact with the tool and these can be levelled by applying little force, thus reducing friction. After levelling the structure, there is no longer any influence on friction.

4 Coating development and characterization

The objective of the development of self-lubricating PVD coatings for the achievement of a dry cold bulk metal forming of steel by means of full forward impact extrusion, is the synthesis of tool coatings, which combine high wear resistance with low friction. Furthermore, the coatings have to be designed depending on the load collective changing over the complex tool geometry. Accordingly, higher mechanical properties are required along the reduction shoulder, for example, to improve wear resistance, since this is where the highest loads occur. Two different coating unit configurations were investigated within of the coating development, see section 2.

4.1 Development of coating system HPPMS CrAlN+Mo:S

Within the scope of the first process and coating development using the HPPMS technology, the focus was on the identification of suitable process parameters. The aim is to find an appropriate chemical composition that simultaneously offers high wear resistance and low friction. CrAlN should provide wear protection, while the Mo and S serves the purpose of friction reduction. A special target was applied during the

deposition, which consisted of two sections - a CrAl20 half and a MoS_2 half, both in form of triangles, see Fig. 10.

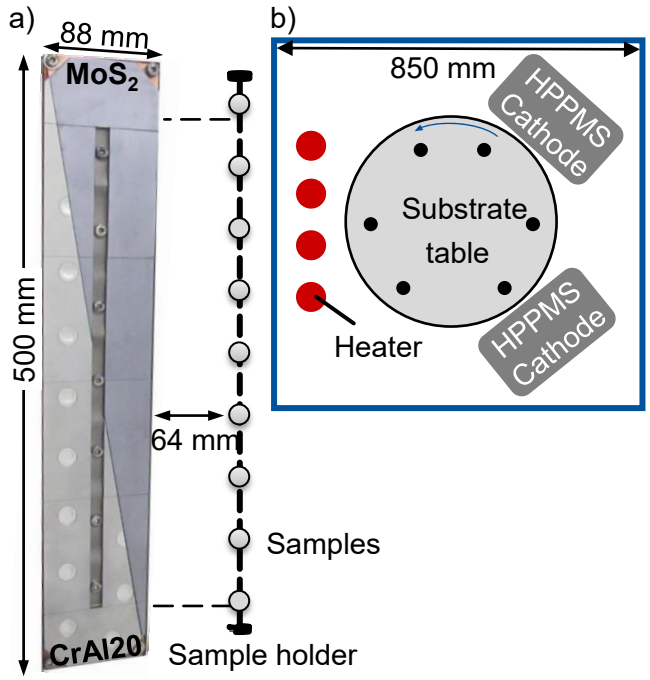

Tab. 2: HPPMS CrAlN+Mo:S coating process parameters

Parameter	Unit	HPPMS CrAlN+Mo:S
Pressure p	mPa	470
Ar flux j(Ar).	sccm	200
N_2 flux $j(N_2)$.	sccm	Pressure controlled
Bias voltage U_{Bias}	V	-120
Cathode Power P	kW	3.5
Pulse frequency f	Hz	500
Pulse length t_{on}	µs	200

Fig. 10: Illustration of the custom triangular target (a) and schematic the coating unit and target configuration (b)

The CrAl20 half consists of a Cr-base plate with ten Al-plugs of diameter $Ø_{Al} = 15$ mm with a purity of $x_{Cr} = 99.9$ at.% and $x_{Al} = 99.5$ at.%. The MoS_2 target section had a purity of 99.5 at.%. Several substrates at different positions on the holder were coated along the modified target, thus these specimens have a variation of the chemical composition. The coating process parameter used are listed in Tab. 2. The nitrogen gas flow was controlled over the total pressure of $p = 470$ mPa. Deposition temperature at substrate was kept below annealing of temperature of the substrate material AISI D2. During deposition, the samples were rotated in a two folded rotation.

The chemical composition of the coatings as a function of the sample position to the triangular target is shown in Fig. 11. A decrease of the Al and Cr contents of the coatings can be observed with the increasing position of the sample in the holder in the coating deposition setup. The Cr content decreases about $\Delta x_{Cr} = 15.1$ at.% from $x_{Cr} = 47.1$ at.% to $x_{Cr} = 32.0$ at.%. The Al content drops from $x_{Al} = 17.4$ at.% to $x_{Al} = 9.5$ at.% in. However, both the Mo and S contents increase with the increasing position of the sample in the holder. The highest sample of the holder contains almost ten times more of S $x_S = 22.3$ at.% comparing to the lowest mounted specimen with $x_S = 2.2$ at.%. The Mo content increases by $\Delta x_{Mo} = 16.0$ at.% from $x_{Mo} = 5.2$ at.% to $x_{Mo} = 21.2$ at.%. These developments in the chemical compositions are associated to the triangular target setup as seen in Fig. 10. The analysis of the chemical composition shows that there is no stoichiometric composition of MoS_2 as provided by the target. During coating deposition, also a resputtering of the deposited coating material on the substrate takes place, which is mainly caused by accelerated argon ions [43–45].

In particular, due to the comparable atomic weights of argon and sulfur, the resputtering effect of sulfur must be taken into account, as the atomic mass has a significant influence on this effect. The energy transfer of an incident atom E_{inc} to a stationary atom E_{sta} is described by the transfer-energy equation [46].

$$\frac{E_{inc}}{E_{sta}} \propto \frac{4M_{inc}M_{sta}}{(M_{inc}+M_{sta})} \tag{1}$$

This equation describes the ratio of the kinetic energy transferred from a moving particle E_{inc} to a stationary particle E_{sta}. The transmitted energy ratio is at maximum if the molar mass of the incident atom m_{inc} is equal to the molar mass of the stationary atom m_{sta}. In the case of sulfur and argon, the molar masses are closely adjacent to each other with $M_{Ar} = 39.95$ g/mol and $M_S = 32.07$ g/mol, therefore a removal of already condensed sulfur atoms is more probable than those of the other coating elements.

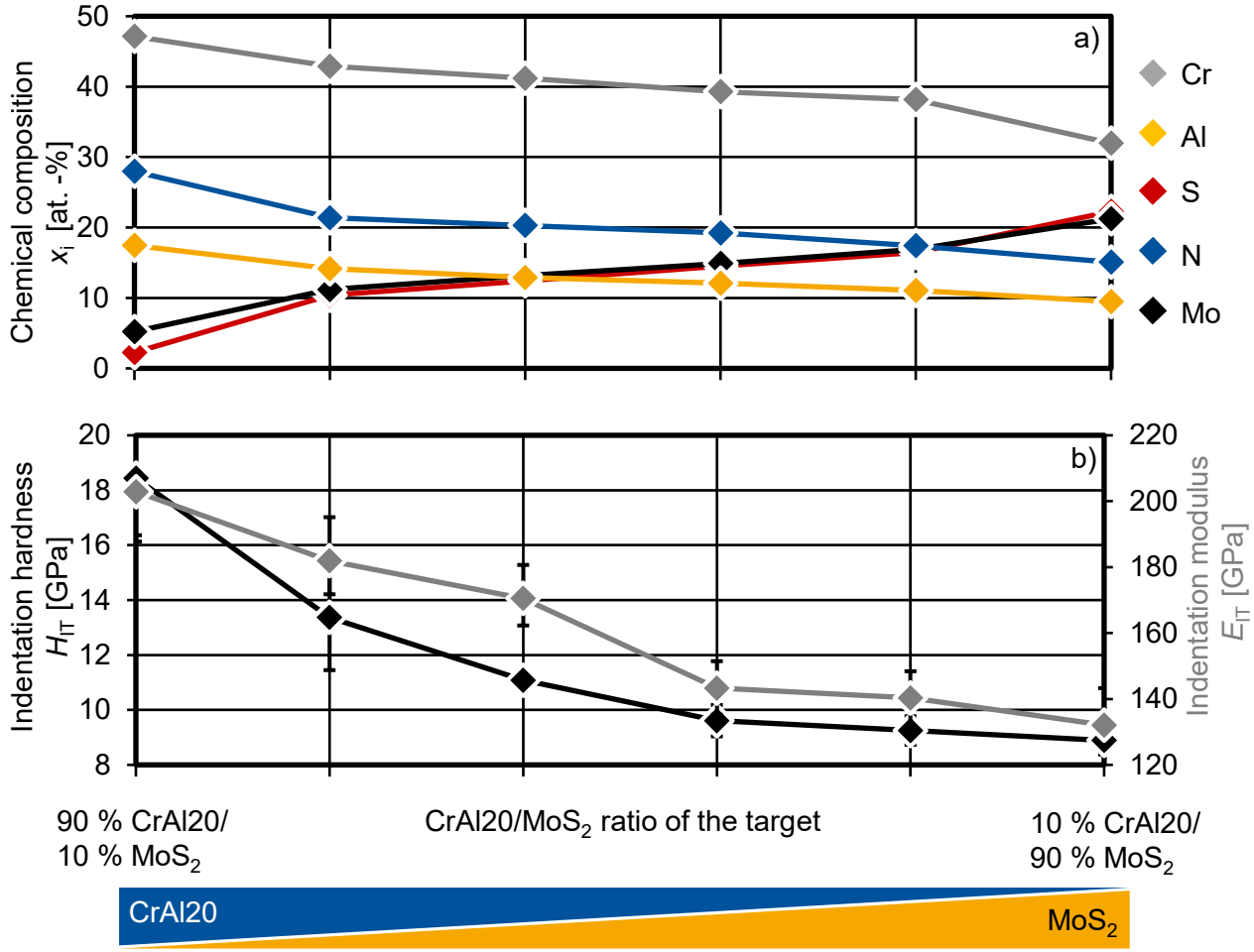

Fig. 11: Chemical composition by means of GDOES (a) and mechanical properties indentation hardness and indentation modulus as a function of substrate position in front of the triangular target [47]

When considering the mechanical properties as a function of the chemical composition, it can be seen that the indentation hardness and the indentation modulus decrease significantly with increasing Mo and S content. The highest indentation hardness is H_{IT} = (18.4±2.3) GPa at a Mo+S content of x_{Mo+S} = 7 at.%. The lowest indentation hardness is H_{IT} = (8.9±0.5) GPa at a Mo+S content of x_{Mo+S} = 42 at.%. This is due to the decreasing content of the CrAlN hard phase and is in accordance with the findings explained in the state of the art of the introduction.

To investigate the influence of the chemical composition on the tribological behavior, model tests were carried out using PoD tribometer. Fig. 12 shows the coefficient of friction *CoF* of the coatings as well as the uncoated substrate AISI D2 as reference against a counterpart pin consistent of the material AISI 5115 which was selected because the case-hardening steel AISI 5115 is one of the typical workpiece materials in cold bulk metal forming [39]. The uncoated substrate shows almost constant friction behavior after the run-in process with a coefficient of friction of *CoF* ≈ 0.75. The coating with x_{Mo} = 8.1 at.% and x_S = 6.5 at.% exhibits the lowest coefficient of friction. The *CoF* after a running-in phase is *CoF* = 0.28.

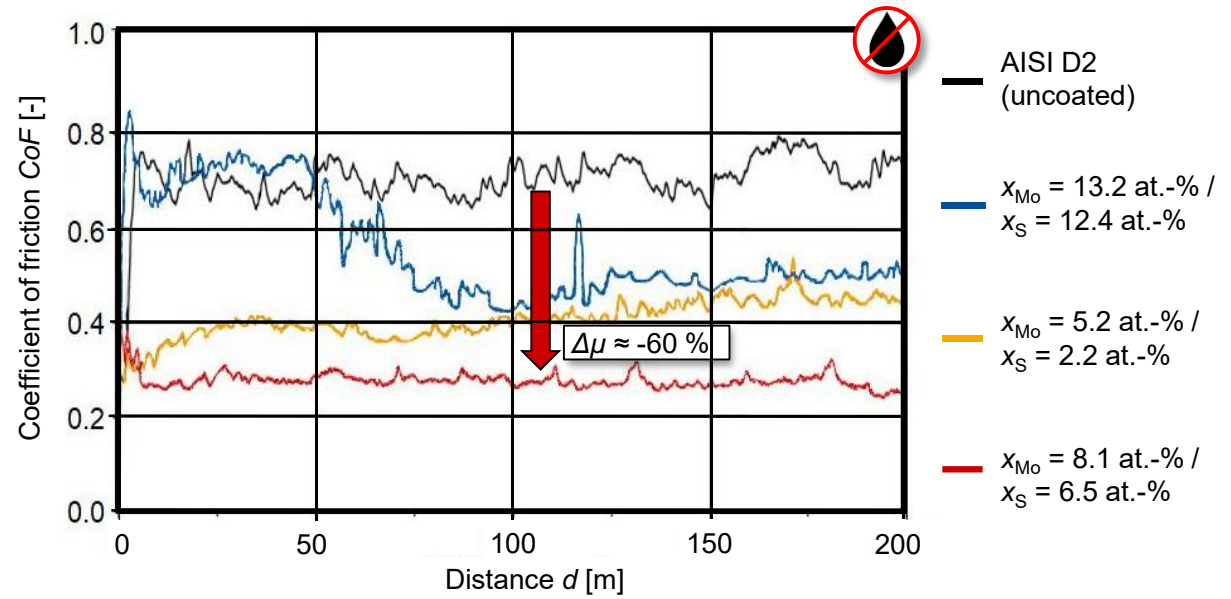

Fig. 12: Coefficient of friction of the HPPMS CrAlN Mo:S coated specimen in dependency of the Mo- and S-content and the uncoated AISI D2 substrate against AISI 5115 counterpart in PoD tribometer [47]

In addition to the test results presented here, the same analyses were performed to characterize the coating properties and tribological behavior of the CrAlN coating variants modified with W and S instead of Mo and S. The results published in [48–50] reveal comparable mechanical properties depending on the chemical composition. Furthermore, similarly low coefficients of friction were determined in PoD tests.

4.2 Development of dcMS/HPPMS coating system hybrid CrAlN+Mo:S

Based on the knowledge of process and coating development using HPPMS technology and the concept of triangular targets to produce different coating systems with varying chemical compositions, the coating concept was further developed using the dcMS/HPPMS hybrid technology. The advantage of this deposition technology is the increased economic efficiency of the deposition process due to a higher deposition rates compared to the HPPMS technology. A schematic illustration of the coating chamber is shown in Fig. 13.

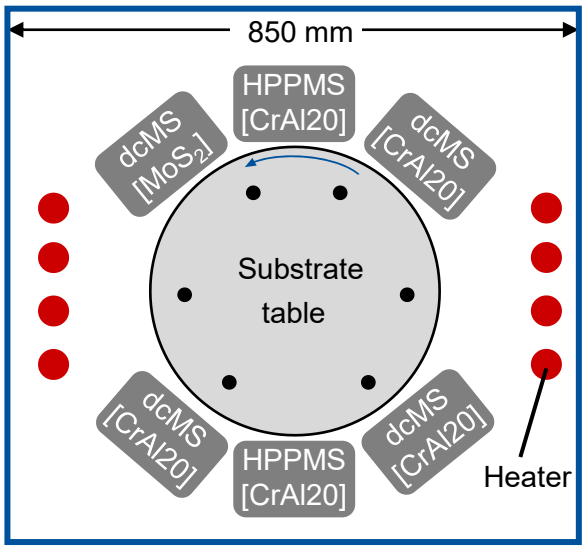

Fig. 13: Schematic illustration of the coating camber in top view [23]

Tab. 3: Hybrid CrAlN+Mo:S coating deposition parameters

Parameter	Unit	dcMS/HPPMS CrAlN+Mo:S
Pressure p	mPa	710
Ar flux j(Ar).	sccm	200
N_2 flux $j(N_2)$.	sccm	Pressure controlled
Bias voltage U_{Bias}	V	-100
Cathode Power $P_{HPPMS\text{-}CrAl20}$	kW	5
Cathode Power $P_{dcMS\text{-}CrAl20}$	kW	3
Cathode Power $P_{dcMS\text{-}MoS2}$	kW	2
Pulse frequency f	Hz	500
Pulse length t_{on}	µs	40

Five CrAl20 targets and one MoS_2 target mounted on a dcMS cathode were used for the deposition of the coatings. This target configuration ensures a similar chemical composition of the coatings, which have shown promising tribological properties in previous investigations. The process parameters for producing the coating systems presented below are listed in Tab. 3. The coating systems synthesized by the hybrid process

were deposited in a one-folded rotation. This leads to the formation of a nanolaminate coating architecture, which is characterized by improved mechanical properties.

Fig. 14 shows a schematic illustration of the coating concept, Fig. 14 (a), a scanning transmission electron microscopy (STEM) image of the composite consisting of the substrate material AISI D2, a metallic bond coat CrAl, a nitride interlayer CrAlN and a toplayer CrAlN+Mo:S. Fig. 14 (b).

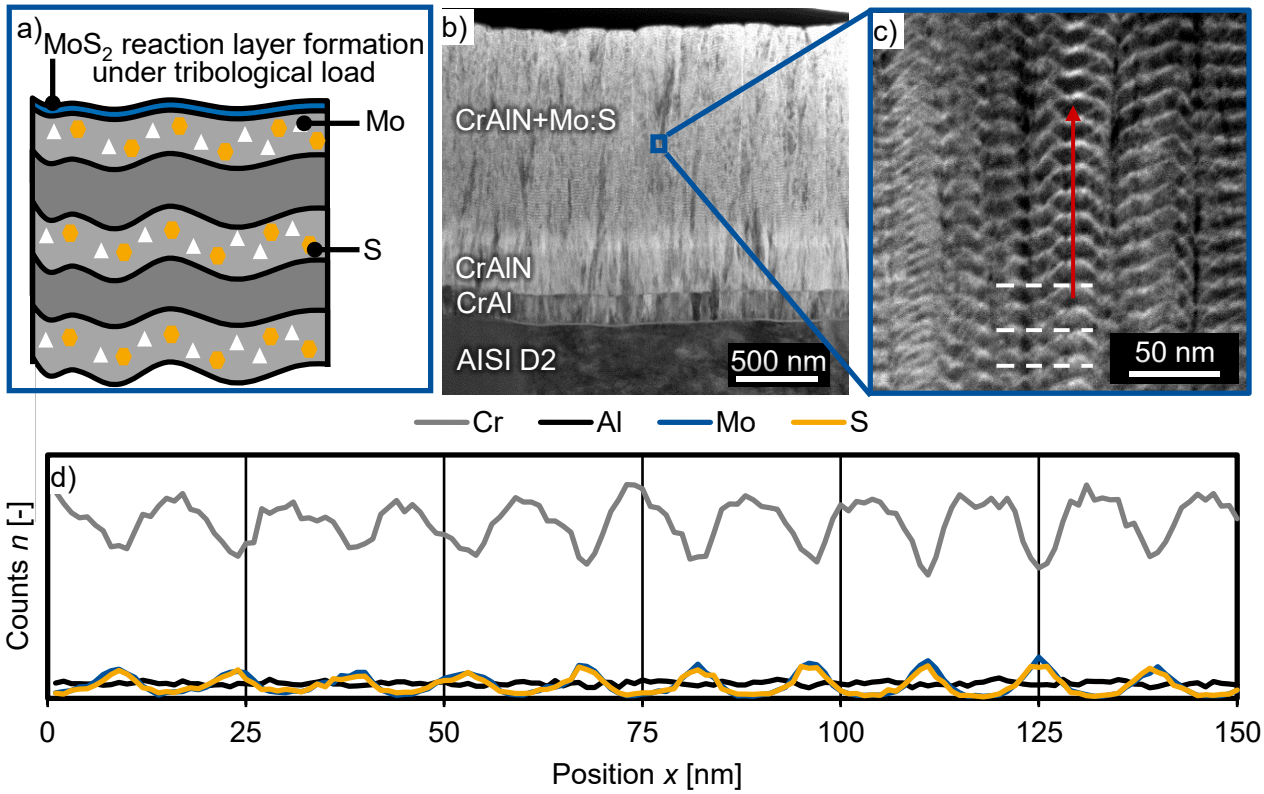

Fig. 14: Schematic of coating concept (a), cross-sectional STEM BF image of the coating hybrid CrAlN+Mo:S (b), STEM high-angle annular dark field image with higher magnification (c) and EDS linescan spectrum along the red arrow (d) [23]

An enlarged section of the top layer of a STEM high-angle annular dark field (HAADF) micrograph is illustrated in Fig. 14Fig. 2 (c) and an EDS linescan along the individual layers of the nanolaminate coating architecture is in Fig. 14 (d). The coating thickness is approximately $s = 2$ µm. To improve the compound adhesion between coating and substrate, a metallic bond coat and a nitride interlayer were first deposited, see Fig. 14 (b). Rockwell indentation tests show that after indentation with a force of $F = 1{,}372.93$ N, no spallings or cracks are visible at the edge of the Rockwell indentation. Thus, the adhesion strength after the Rockwell indentation test can be assigned to the best adhesion class of HF1. Images of the Rockwellindents are published in [23]. Quantification by means of the scratch test reveals high critical scratch loads of $L_{C2} = 60$ N and $L_{C3} = 90$ N, which corresponds to high adhesion of the coating to the substrate. The nanolaminate architecture of the top layer CrAlN+Mo:S, which is caused by the one-folded rotation of the substrates, can be seen with a higher magnification factor in the STEM HAADF micrograph, Fig. 14 (b). The periodicity of the nanolayers ranges from $\Lambda = 12$ nm to $\Lambda = 15$ nm. Along the red arrow with a length $l = 150$ nm, Fig. 14 (c), a drift corrected EDS-linescan was performed to determine the chemical composition of the individual nanolayers. The EDS-linescan reveals that the dark regions present the CrAl-rich and the bright regions present the Mo- and S-rich nanolayers. As shown in the schematic diagram of the coating system, no discrete individual nanolayers containing CrAl and Mo+S are present, but only individual layers that contain or do not contain Mo and S. Furthermore, electron diffraction analyses in TEM and XRD analyses have shown that no crystalline phases of MoS_2 are detectable. This suggests that the molybdenum and sulfur are not present as a chemical compound, which is, however, desirable with regard to mechanical properties and wear resistance. Otherwise, the soft S-Mo-S planes would shear off under tribological stress and the functional layer would wear rapidly.

The chemical composition of the coating hybrid CrAlN+Mo:S was determined by EPMA. Tab. 4 shows the element content and ratio of x_S/x_{Mo}. The chemical analysis reveals that the Cr content is the highest with $x_{Cr} = 38.6$ at.%. The Al and Mo contents are $x_{Al} = 4$ at.% and $x_{Mo} = 4.4$ at.%. The S to Mo ratio is, like the

previously analyzed HPPMS coatings, sub-stoichiometric with $x_S/x_{Mo} = 34.1$ at.%. This can be explained by increased resputtering of the already deposited S atoms, since only one MoS2 target is used with five CrAl20 targets operated simultaneously. Further investigations reveal a further decrease of the sulfur to molybdenum ratio x_S/x_{Mo} with increasing bias voltage U_{bias}, which is due to the increased kinetic energy of the impinging Ar ions and the associated increased resputtering [46].

Tab. 4: Chemical composition of coating system hybrid CrAlN+Mo:S by means of EPMA [23]

	Element conent [at.%]					S/Mo [%]
	Cr	Al	N	Mo	S	
CrAlN+Mo:S	38.6	4.0	51.5	4.4	1.5	34.1

To determine the mechanical properties, analyses were carried out using nanoindentation. The indentation hardness is $H_{IT} = (23.2 \pm 1.2)$ GPa and the indentation modulus is $E_{IT} = (317.6 \pm 20.0)$ GPa. The investigations were repeated after thermal ageing at $T = 250$ °C with a holding time of t = 48 h, as FEM simulations have shown that these temperatures occur during dry full forward impact extrusion [41]. No influence of annealing could be determined. The arithmetic mean roughness of the coating is $Ra = 0.02$ µm. The tribological behavior of the coated samples was investigated in model tests without the use of externally supplied lubricants. For this purpose, tests were carried out using PoD at $RT = 23$ °C and $HT = 250$ °C with a counter body consisting of the material AISI 5115. The coefficient of friction of the uncoated substrate materials AISI D2 and the hybrid CrAlN+Mo:S coating are shown in Fig. 15 (a). A significant reduction of the *CoF* due to the self-lubricating coating was achieved at *RT* and *HT*. In comparison of the uncoated reference to the coated sample at *HT* conditions, a reduction of friction by $\Delta CoF = 70$ % could be achieved, see Fig. 15 (a).

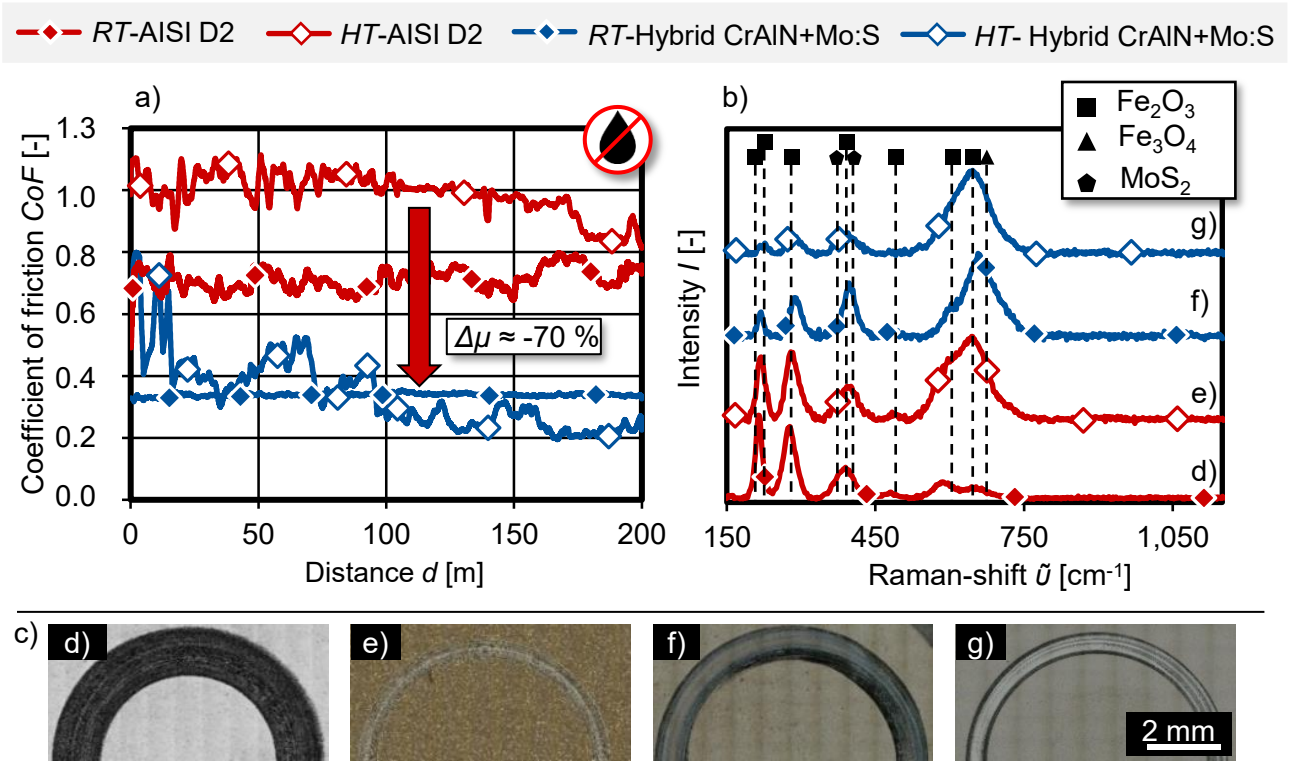

Fig. 15: Coefficients of friction of uncoated and hybrid CrAlN+Mo:S coated substrate materials AISI D2 by PoD at RT and HT (a), Raman spectra within the wear tracks (b) and CLSM images of the wear tracks (c) [51]

The characterization of the tribochemically induced reaction layer formation within the wear track is based on the Raman spectra shown in Fig 15 (b). For this purpose, the uncoated reference AISI D2 and the Hybrid CrAlN+Mo:S coated specimen were examined after the PoD tests at RT and HT respectively. The peaks of the Raman shifts $\tilde{\upsilon} = 223$ cm^{-1}, $\tilde{\upsilon} = 230$ cm^{-1}, $\tilde{\upsilon} = 293$ cm^{-1}, $\tilde{\upsilon} = 404$ cm^{-1} and $\tilde{\upsilon} = 603$ cm^{-1} and the low intensity peaks at $\tilde{\upsilon} = 648$ cm^{-1}, $\tilde{\upsilon} = 498$ cm^{-1} are haematite (Fe_2O_3) [52,53]. Magnetite (Fe_3O_4) is detected by a peak at $\tilde{\upsilon} = 675$ cm^{-1} [52,53]. Two peaks between 383 cm$^{-1} \leq \tilde{\upsilon} \leq 408$ cm^{-1} are characteristic for the presence of MoS_2 [54].The Raman spectra show an increased formation of hematite and magnetite due to tribo-oxidation of the Fe containing counterbody and the uncoated reference AISI D2. These iron oxides are also deposited in the wear marks of the coated samples. Furthermore, after the PoD tests at *HT*, an increased intensity of the

magnetite related peaks is visible. The increased intensities of the respective peaks at 383 $cm^{-1} \leq \tilde{\upsilon} \leq 408$ cm^{-1} in both coated samples indicate the formation of the solid lubricant MoS_2 under tribological stress, but the two peaks characteristic for MoS_2 are superimposed by an intermediate hematite peak. The significant friction reductions achieved with the applied self-lubricating coatings indicate the formation of the solid lubricant originating from the elements Mo and S under tribological stress.

In addition to the test results presented here, further analyses were performed to characterize the coating properties and tribological behavior of the CrAlN coating variants modified with W and S instead of Mo and S presented in [55]. The hybrid CrAlN+Mo:S coating system shows significantly higher compound adhesion to the substrate material AISI D2 compared to the tungsten modified coating system. Furthermore, the molybdenum and sulfur modified CrAlN coatings exhibit improved friction-reducing properties. In addition to the cold work steel AISI D2, the same investigations were also carried out with the high speed steel AISI M2 published in [23]. In conclusion, the compound adhesion of the coating system hybrid CrAlN+Mo:S to the substrate AISI D2 is slightly better compared to the substrate AISI M2. Furthermore, the tribological behavior of the compound hybrid CrAlN+Mo:S/AISI D2 is better than the compound CrAlN+Mo:S/AISI M2, particularly under high temperature conditions.

4.3 Plasma-diagnostic investigations as a function of the complex inner tool geometry

In order to obtain a better understanding of the coating deposition within the complex inner geometry of two-shoulder forming dies, plasma diagnostic tests were carried out using OES. To investigate the influence of the complex tool geometry on the resulting coating properties, an experimental tool model with the same dimensions was developed and manufactured. This model has three holes with a diameter of $\varnothing = 10$ mm, which corresponds to the diameter of the beam diameter detectable by the collimator. These holes were placed equidistantly at the beginning, in the middle and at the end of the tool to investigate the influence of the higher aspect ratios on the plasma properties. These three holes are each located on the ahead inlet area, middle inlet area and behind outlet area of the two-shouldered die, see Fig. 5.

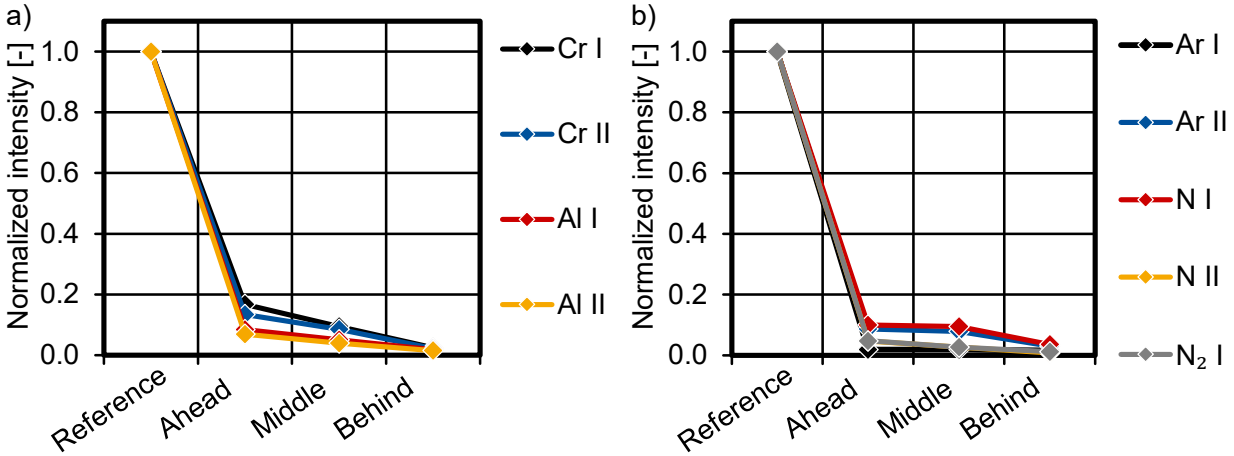

Fig. 16: Normalized intensities of metallic (a) and gaseous (b) plasma species as a function of position along the two-shouldered inner contour of the die from ahead inlet area to middle inlet area to outlet area acquired in front of a HPPMS CrAl20 target

When comparing the normalized intensities of all species within the inner contour of the die to the reference measurement position, a significant decrease can be seen, Fig. 16. This is in line with the expected results due to the small diameter of the inner contour of the die. Furthermore, as the aspect ratio increases from start to end along the die, a further decrease in intensity can be observed. This is due to the line of sight characteristic of PVD processes during coating deposition. When looking at the metal species, it can be seen that on the one hand the intensities of the Cr species are higher than those of the Al species. This is due to a strongly increased Cr to Al content of the target used. In addition, the intensities of the excited Cr I and Al I species are higher compared to the single ionized Cr II and Al II species, which is due to the fact that the ions are accelerated by the negative substrate bias voltage in the direction of the substrate compared to the excited species and encounter the substrate surface at an early stage.

With the exception of Ar, the gas species behave analogously. Why the intensity of Ar II is higher than that of Ar I is currently being investigated in more detail. This investigation method was also performed in front of a CrAl20 target and a MoS_2 target which were running with the dcMS technology. The results are comparable to those presented here.

4.4 Transfer of the coating concept for application to the forming tools

For the investigations on the coating thickness distribution along the longitudinal axis of the 2-shouldered forming die, the coated specimen positioned at P1 to P5 of the experimental tool were considered, Fig. 17. For this purpose, an experimental model of the die was designed and manufactured in order to analyze the coating deposition as a function of the complex inner geometry of the forming die.

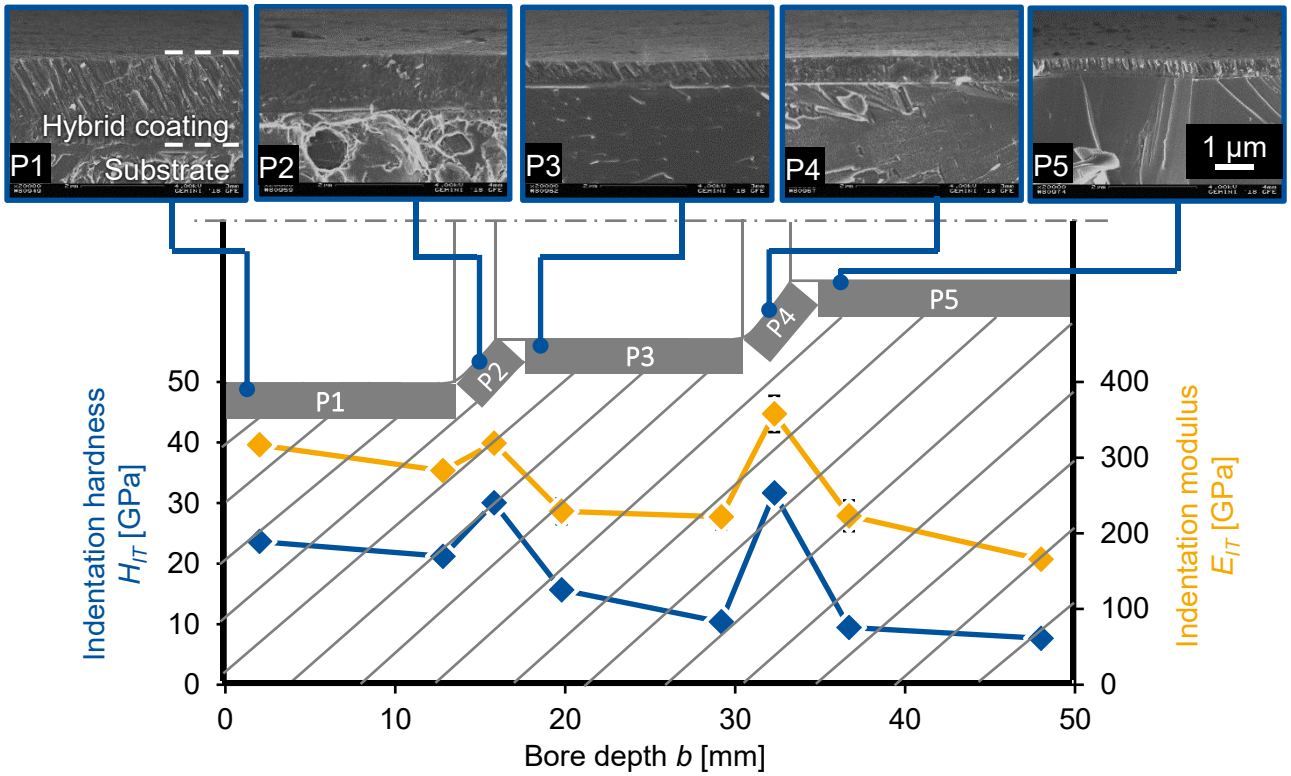

Fig. 17: SEM cross section images of the coating hybrid CrAlN+Mo:S positioned at P1 to P4 at the inner of the bore hole along the longitudinal axis of the experimental tool

The die model exhibits the same dimensions as the real two-shoulder die. However, a notch has been cut along the die to mount five samples along the inner contour of the die. This has the advantage that a real die does not have to be cut for coating analysis. The front and rear sections of the samples were analyzed by SEM with respect to morphology and by nanoindentations to determine the mechanical properties. Fig. 17 shows the SEM cross section fractures and the mechanical properties of the applied coating system hybrid CrAlN+Mo:S. The SEM images indicate that the entire length of the experimental tool is coated throughout the inner contour of the bore hole. Due to the PVD characteristic line-of-sight deposition, the coating thickness decreases with increasing bore depth. These results are in accordance with the results of the plasma-diagnostic OES investigations. Furthermore, the morphology of the coating differs slightly as a function of the bore depth of the die. In this regard, the sample located in the front side of the experimental tool at position P1 reveals the maximum deviation from a vertical orientation of coating's columns, which will be generally observed for the samples located parallel to the targets in coating unit. The microstructural columns at P1 exhibit an orientation of $\theta = 50°$. By a change in the orientation of substrate's surface with respect to the targets, the coating at P2 and P4 exhibits a fine and dense morphology. Within the position P3 and P5, the morphology changes again to a columnar microstructure. However, the inclination of the columns approaches gradually decline to $\theta = 90°$ along the longitudinal axis of the experimental tool from P3 to P5 due to the bias voltage.

Examining the mechanical properties as a function of the bore depth, it can be seen that the highest mechanical properties with $H_{IT} = (30.0 \pm 2.7)$ GPa are present at the impact reduction shoulders. This is advantageous considering the resistance to abrasive wear, since the highest loads occur at the forming shoulders. In the inlet area which corresponds to P1, the indentation hardness is $H_{IT} = (23.6 \pm 2.2)$ GPa. The mechanical properties decrease with increasing bore depth, but this is unproblematic due to lower present loads. The same investigations were also carried out with a one-shoulder die model when considering four different hybrid CrAlN+Mo:S and hybrid CrAlN+W:S coatings.

The influence of the used bias voltage on the coating thickness distribution was examined. The coating variants deposited with tungsten instead of molybdenum exhibit an increased deposition rate by $\Delta ds/dt \approx 15$ %. Furthermore, the influence of the refractory metal Mo and W on the mechanical properties, coating morphology, adhesion to the substrate material and tribological behavior was investigated shown in [55]. Based on the investigations of the coating deposition on complex inner geometries using the developed die models, it could be shown that the entire inner surface of the forming dies can be coated throughout. Furthermore, the high mechanical properties, especially along the reduction shoulder, as well as the promising frictional behavior in model tests, meet the requirements for tool coating for the achievement of dry full forward impact extrusion. For this reason, the coating system hybrid CrAlN+Mo:S was applied to the real, one- and two-shoulder forming dies. In order to ensure a sufficient coating thickness, the coating duration was extended to $t = 100$ min.

5 Interaction between workpiece surface structure and PVD tool coating by tribological model tests

In order to investigate the tribological behavior of the self-lubricating coatings in tribological contact with different surface structures, ring compression tests were conducted. The test setup and evaluation is analogous to the ring compression tests of section 3.1. Therefore, the hybrid CrAlN+Mo:S coating system was applied to the upsetting tools. Due to the self-lubricating properties, the friction factor m determined could be significantly reduced compared to the uncoated upsetting tools [42].

Furthermore, dry PoC tests were carried out to analyze the influence tool-sided approach of the self-lubricating PVD coatings in tribological interaction of the workpiece-sided approach of various surface structures on the tribological behavior at elevated temperatures of $T = 250$ °C and high normal force of $F_N = 2{,}600$ kN. Fig. 18 presents the apparent coefficient of friction CoF^*, which correspondents to the ratio of normal force to the resulting tangential force, as a function of the distance.

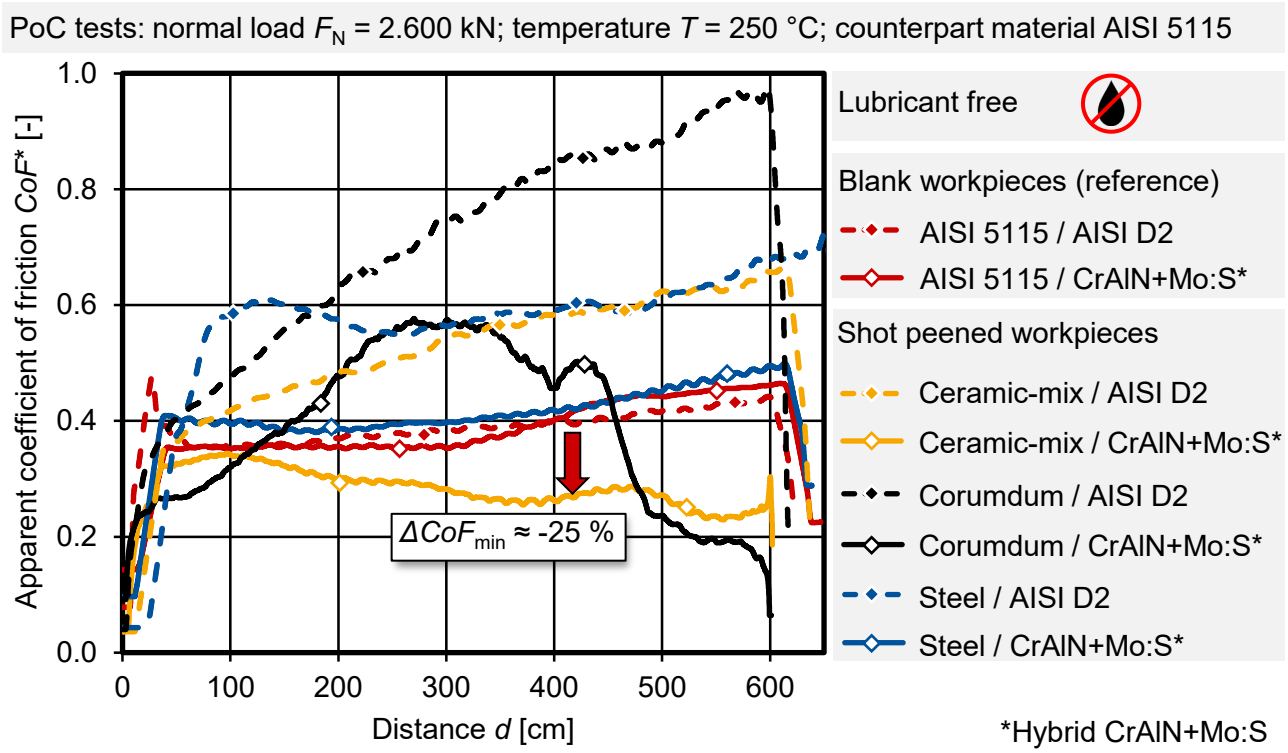

Fig. 18: Apparent coefficient of friction CoF^* as a function of the distance, cylinder surface structure and coated as well uncoated pins in dry pin-on-cylinder tests

The apparent CoF^* has been used because the high normal force applied led to plastic deformation of the cylinder. The tests were carried out in the same way as in section 3.1, but on the one hand a special temperature control device was developed to take into account the influence of the temperature of $T = 250$ °C which occurs in full forward impact extrusion. On the other hand, the promising coating system CrAlN+Mo:S was examined in comparison to uncoated pins with regard to friction and wear behavior as a function of the surface structure. The investigations reveal that the CoF^* can be reduced by the self-lubricating coatings in combination of all three surface structures compared to the uncoated pins. The combination of a ceramic-mix-peened structure and a coated pin shows the most favorable frictional properties. The CoF^* was reduced

by ΔCoF^* = -25 % compared to the best uncoated combination. It can also be seen that the CoF^* of the coated pin tested against the corundum-peened structure exhibits the lowest friction up to a distance of d = 100 cm. The investigations reveal that the CoF* can be reduced by the self-lubricating coatings in combination of all three surface structures compared to the uncoated pins. The combination of a ceramic-mix-peened structure and a coated pin shows the most favorable frictional properties. The CoF^* was reduced by ΔCoF^* = -25 % compared to the best uncoated combination. It can also be seen that the CoF^* of the coated pin tested against the corundum-peened structure exhibits the lowest friction up to a distance of d = 100 cm. As a result of increasing wear, which is noticeable as adhesive wear of the counterpart material, there is no longer a self-lubricating effect. As a result of the further course of the test, the CoF^* drops again, which is very probably due to the loosening of these cold welds and the self-lubricating effect of the coating becomes effective again. The CoF^* curves of the uncoated pins with the three surface structures show that very poor friction conditions exist in the tribological system of the PoC, especially against the corundum peened surface.

This is due to significant adhesive wear of the uncoated pins. Wear analyses of the pins using CLSM reveal that the coated pins exhibit practically no adhesion of the counterpart material, whereas the uncoated pins have significant adhesion. Furthermore, the cross-sectional area of the wear tracks resulting from all uncoated pins is significantly larger than that of coated pins. Analyses of the resulting wear tracks of the cylinders show that, on the one hand, the cross-sectional area of the wear track is significantly smaller compared to the resulting wear tracks of the uncoated pins. Furthermore, the resulting arithmetic mean roughness within the wear track of the coated pins with $Sa \approx 0.4$ µm is significantly lower than that of the uncoated pins with Sa = 2.4 µm at the reference surface. With increasing initial roughness due to the different peening media, an increase in the adhesive wear of the uncoated pins as well as an increase in the roughness of the resulting wear track can be observed.

6 Transferability to the industrial impact extrusion process

The results of the investigations of the self-lubricating tool coatings as well as the surface structures of the workpieces have shown that a reduction of friction is possible with the help of a suitable combination under dry tribological boundary conditions. These results must now be transferred to full forward impact extrusion. To achieve this, a full forward impact extrusion tool was designed and manufactured. It was of great importance that the active elements are divided into segments in order to be able to change the active elements quickly in case of wear or failure of the tool on the one hand and to have not too large aspect ratios for the coating process on the other hand, Fig. 19.

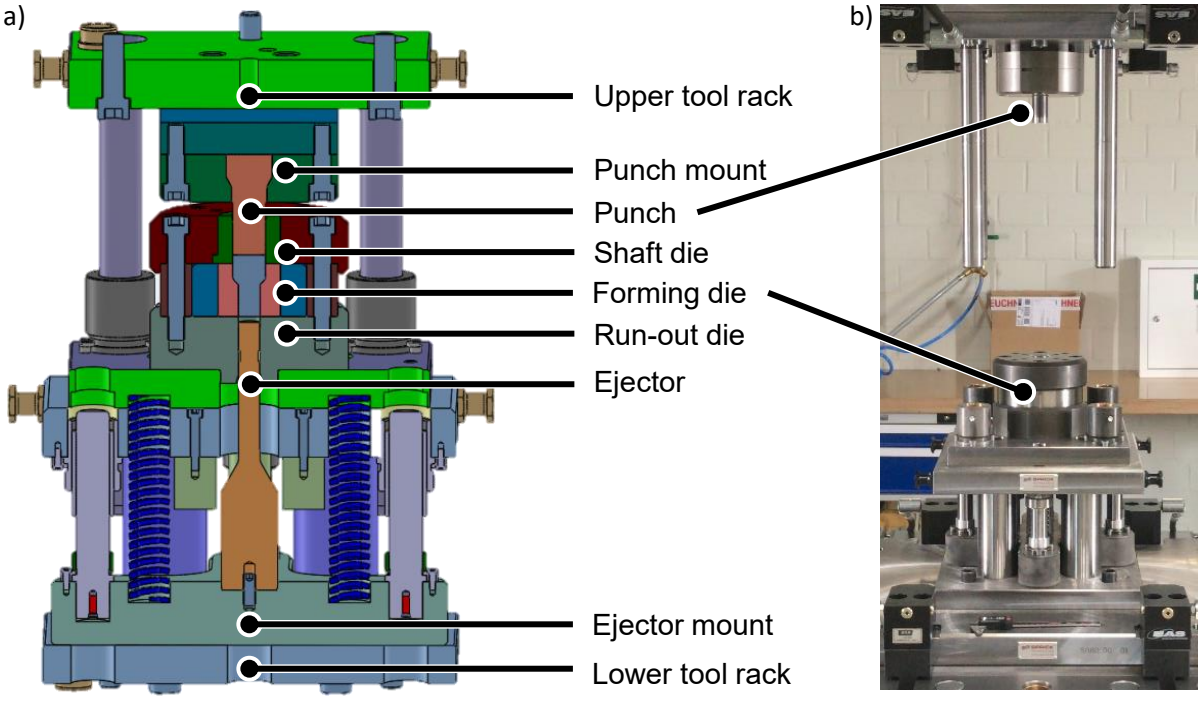

Fig. 19: Tool design for full forward impact extrusion with modular exchangeable shank and forming die

Thus, it is possible to achieve a sufficiently thick coating on the active elements. The workpieces have an initial length of $l_i = 40$ mm and an initial diameter of $d_i = 31.2$ mm. The workpieces are structured in the same way as the tribometer and ring upsetting samples by means of shot peening using ceramic-mix and steel balls and corundum particles. The tool consists of the punch, a shaft die and a forming die. It also includes the necessary periphery for fixing and guiding the active elements. The dies used consist of the cold work steel AISI D2. The shaft die and the inlet area of the forming die have a diameter of $d_s = 31.4$ mm. The reduction to $d_r = 20.6$ mm within the reduction matrix is then achieved via a shoulder opening angle of $\alpha_r = 90°$. Based on the tool geometry and the workpiece size, a press stroke of $s = 18$ mm at a punch velocity of $v_p = 5$ mm/s was selected. The machine required is a hydraulic forming press HPX400 from Schuler with a maximum press force of $F_{p,max} = 4{,}000$ kN.

Based on the promising results of the model tests, which have shown the effectiveness of the tool-sided approach of the self-lubricating tool coating and the workpiece-sided approach of the workpiece structuring, it is necessary to investigate the tribological behavior on an industrial scale. Within the scope of the research project, the aim of the first achievement of full forward impact extrusion of steel under dry boundary conditions shall be achieved. Two different die geometries will be considered, see Fig. 3. First of all, field trials will be carried out on an industrial scale with single-shouldered forming dies, since the expected necessary punch forces are lower than with two-shoulder forming dies. Furthermore, the very first forming tests were carried out using the environmentally friendly lubricant Fuchs WISURA 3368, see Fig. 21, on the one hand in order not to damage any of the components of the tool during the first tests, and on the other hand to show that cold bulk metal forming of the case-hardening steel AISI 5115 by means of full forward impact extrusion can be achieved without previously phosphated workpieces. The tests were then repeated under dry tribological boundary conditions. The progression of the punch forces over time presented in section 6.1 shows the average progression of a total of three strokes, respectively.

6.1 Tribological behavior in one-shouldered field trials

An overview of the one-shouldered field trials depending on the lubrication condition, dry or with the liquid lubricant Fuchs WISURA 3368, coated or uncoated, and the workpiece geometry after one strokes is shown in Fig. 20. The maximum punch force is used to assess the tribological behavior. It can be seen that in the dry as well as in the lubricated system, the self-lubricating coating system hybrid CrAlN+Mo:S as well as the workpiece structure led to a reduction of the maximum punch force of the first stroke, respectively. In both, the lubricated and dry tribological system, the combination of the self-lubricating coating hybrid CrAlN+Mo:S and the corundum-peened workpiece structure achieved the lowest punch force after the first stroke.

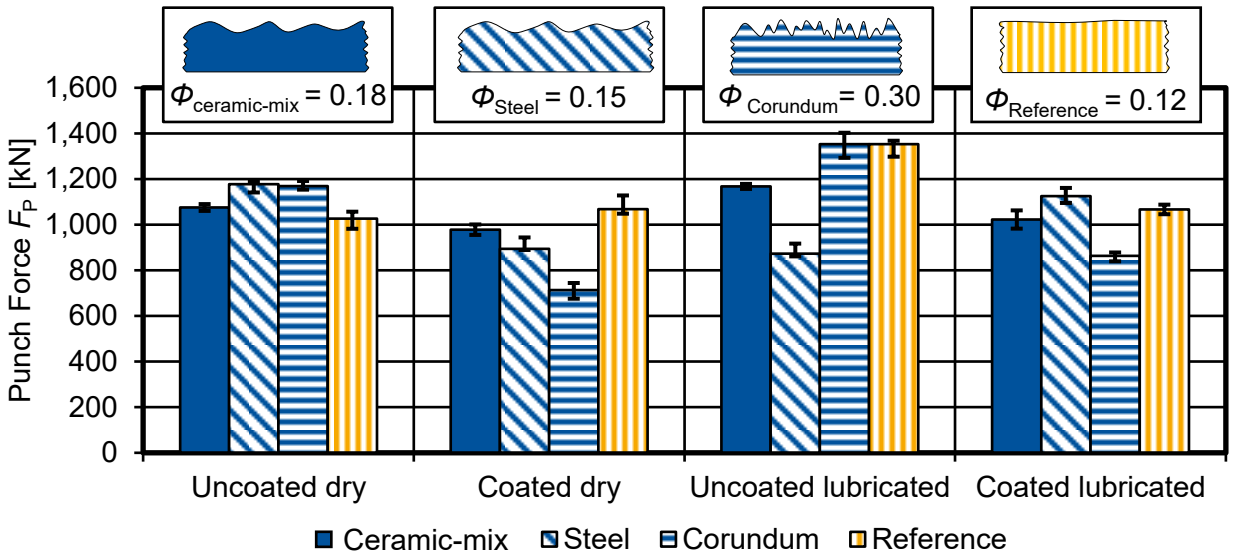

Fig. 20: Mean maximum punch force during full forward impact extrusion depending on the lubrication condition, the tool coating and the surface structures of the workpiece consisting of AISI 5115 after one strokes using one-shouldered forming dies consisting of AISI D2

The results of the single-shouldered field trials after three strokes under lubricated, Fig. 21, and dry boundary conditions, Fig. 22, are presented subsequently. Within initial investigations, the individual surface structures as well as coated and uncoated tools were firstly tested using an environmentally-friendly lubricant. The forces were recorded in the calibrated force shunt using Kistler 9104A force sensors.

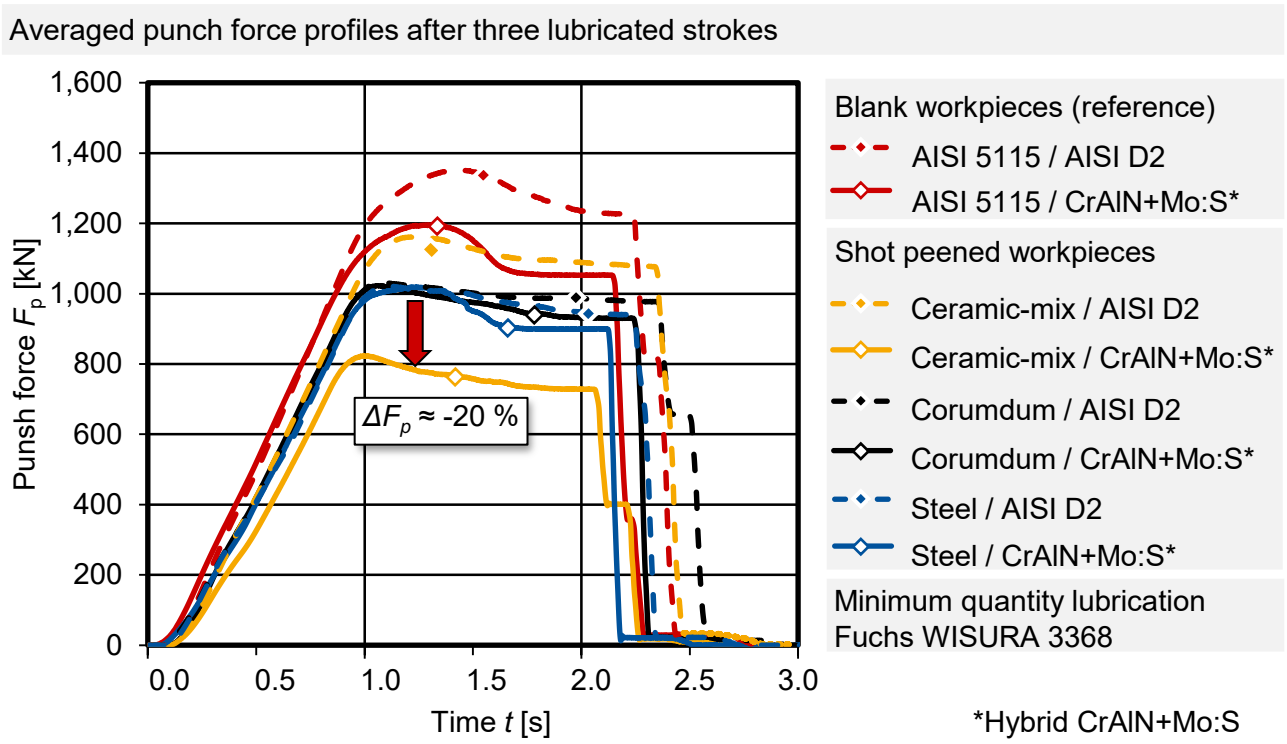

Fig. 21: Force curves of lubricated one-shouldered full forward impact extrusion as a function of the surface structure of the workpiece and the tool coating [56]

The full forward impact extrusion tests show a clear variance to each other. The unstructured reference samples required the highest punch force. This is based on statements of the state of the art according to which a structure on the workpieces offers a possibility of lubricant pockets forming. The lubricants continuously supply the interface between tool and workpiece with lubricant even during the extrusion process, thus continuously reducing friction and ultimately wear in the extrusion process [57]. The smooth reference surface does not have this potential, so that the friction-reducing effect of the lubricant is not present. The highest punch forces of F_p = 1,380 kN were required in contact with an uncoated die. A coated die resulted in a reduction of the punch force to F_p = 1,200 kN against the blank reference surface. The smallest and at the same time the largest change of punch force was achieved by using a workpiece peened with ceramic. In contact with an uncoated die, the punch force was F_p = 1,200 kN, while a coated die resulted in a reduction to a punch force of F_p = 800 kN. The other peened specimens were at about F_p = 1,000 kN between these punch forces and did not differ so significantly. Finally, the effect of the coating is particularly noticeable.

This was followed by the transition to full forward impact extrusion under dry tribological conditions, see Fig. 22. Three samples were extruded for each surface structure and coating condition and the pressing force was averaged. The inlet die was reprocessed due to increasing adhesive wear after each test series depending on the workpiece structure. This ensured that the same boundary conditions were present for all process controls. It can be seen that the use of a coated die resulted in a reduction of the punch forces. The greatest punch force was needed using a workpiece peened with corundum and an uncoated die with F_p = 1,380 kN. The lowest punch force was achieved using the reference surface and a coated die. In this combination a press force of 1,000 kN was achieved. In the absence of lubricants, it was shown that the surface structures have a different influence on friction and thus on the punch force. Rough surfaces, which have the potential to keep more lubricant on the surface and thus reduce friction, are disadvantageous in dry tribological contact with several strokes. The smooth reference surface, on the other hand, leads to a reduction of the punch force. This is due to the flat contact of the workpiece surface on the tool. As a result, the frictional shear stress is reduced from the outset, resulting in lower punch forces. This effect decreases depending on the surface structure. Workpieces peened with ceramic and steel have a slightly rougher surface, but only a slight hardening of the edge zone. In contrast, a sample peened with corundum has the roughest and hardest surface. This also represents the course of the punch forces. The reference surface required the lowest force, then the ceramic peened sample, then the steel peened sample and finally the corundum peened sample as the highest pressing force using a coated die. Besides the influence of the surface structure on the punch force, the influence of the coated dies on the punch force was also shown. On average, a reduction of the punch

force by $\Delta F_p \approx$ -20 % was achieved by using a coated die. The field trials after every three strokes reveal that the surface structure of the workpieces has a significant influence on the adhesive wear. The rougher the workpiece surface, the more pronounced the wear, thus the necessary punch force increases in relation to the number of strokes. The test series with the reference structure shows the smallest increase in punch force.

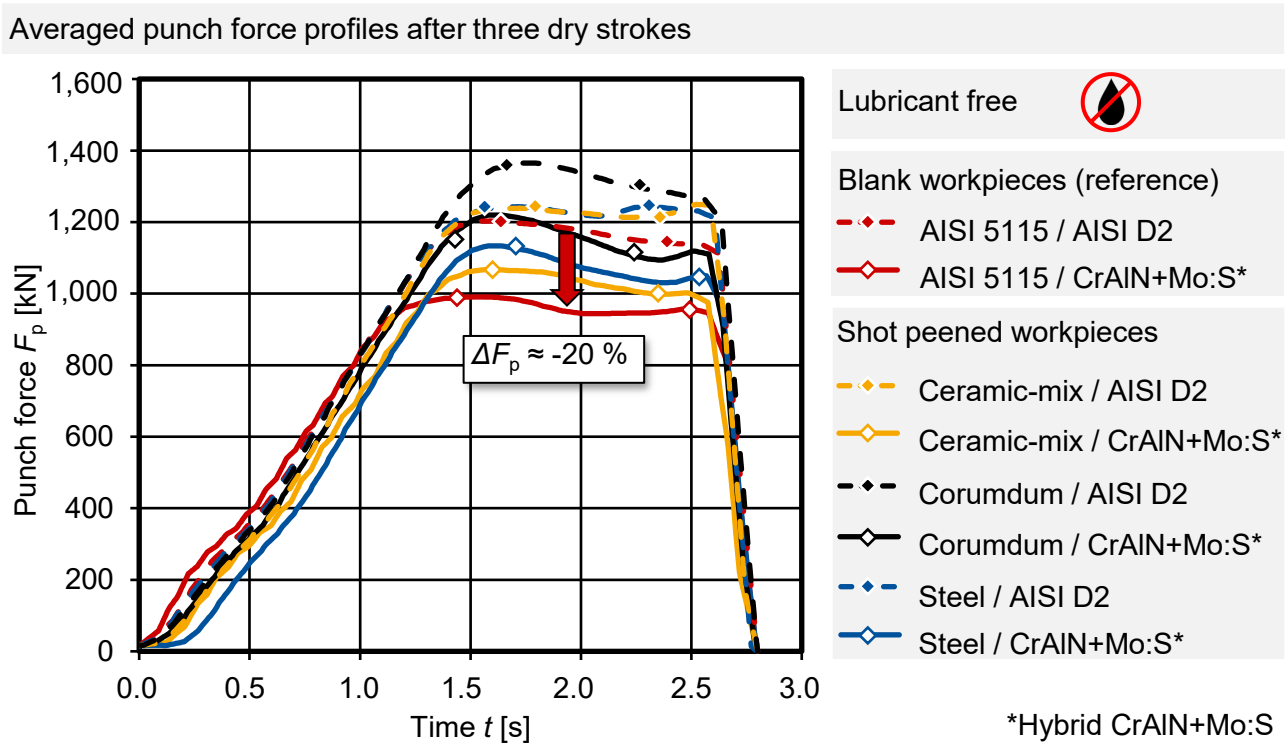

Fig. 22: Force curves of dry one-shouldered full forward impact extrusion as a function of the surface structure of the workpiece and the tool coating [58]

The results of the impact extrusion tests show that the findings of the analogous processes are only partially transferable. Surface textures have the potential to reduce friction and thus the extrusion force by levelling them. This only becomes clear when using lubricant. Under dry tribological boundary conditions the smooth reference surface is the best combination to reduce friction. As was shown in the tests, this is mainly due to wear, which occurs much faster with a surface texture. Subsequent to the dry one-shoulder field trials after three strokes, the forming dies were examined for wear. For this purpose, the four coated dies were cut in pieces and examined along the most heavily loaded area, the reduction shoulder, by means of SEM, Fig. 23. Furthermore, the shaft die was examined by means of camera pictures.

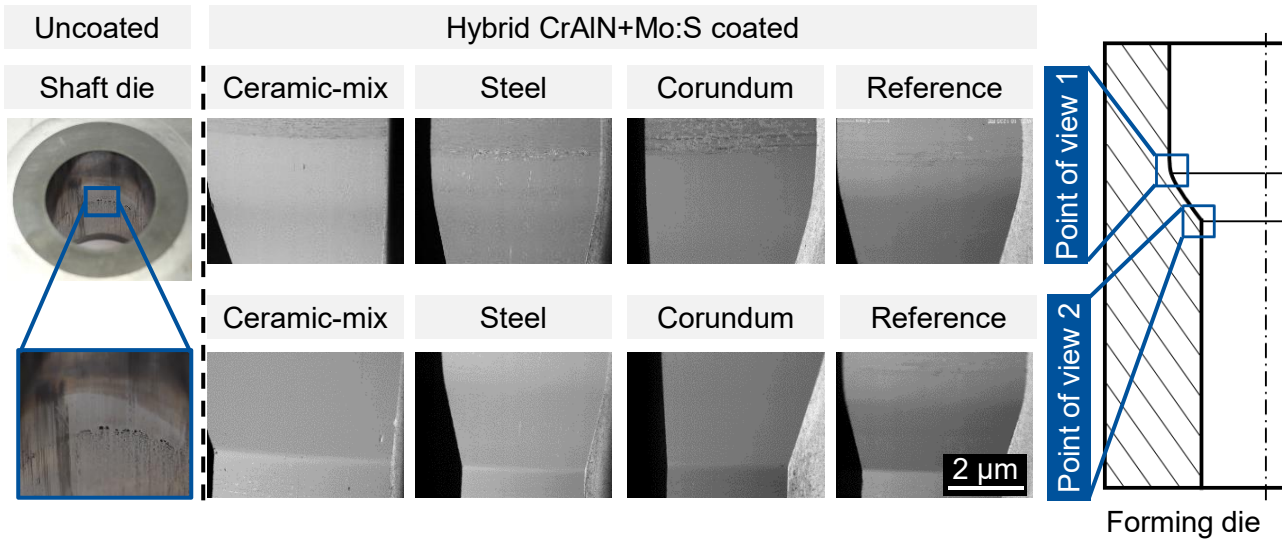

Fig. 23: Signs of wear on the shaft die and on the most heavily loaded area of the forming die [58]

When looking at the SEM images along the outlet area of the reduction shoulder, it can be seen that no wear can be detected independently of the workpiece structure. In the infeed area of the reduction shoulder, the die which was tested with reference workpieces in field trials, shows no visible wear. The dies that were tested with ceramic-mix and steal beads peened workpieces exhibit slight adhesive wear and in comparison to these, the die which was tested with corundum peened workpieces show a slightly more wear. This can be explained by the highest roughness and sharpness of the surface topography of the ceramic peened workpieces. The uncoated forming dies show significant adhesive wear compared to the coated ones.

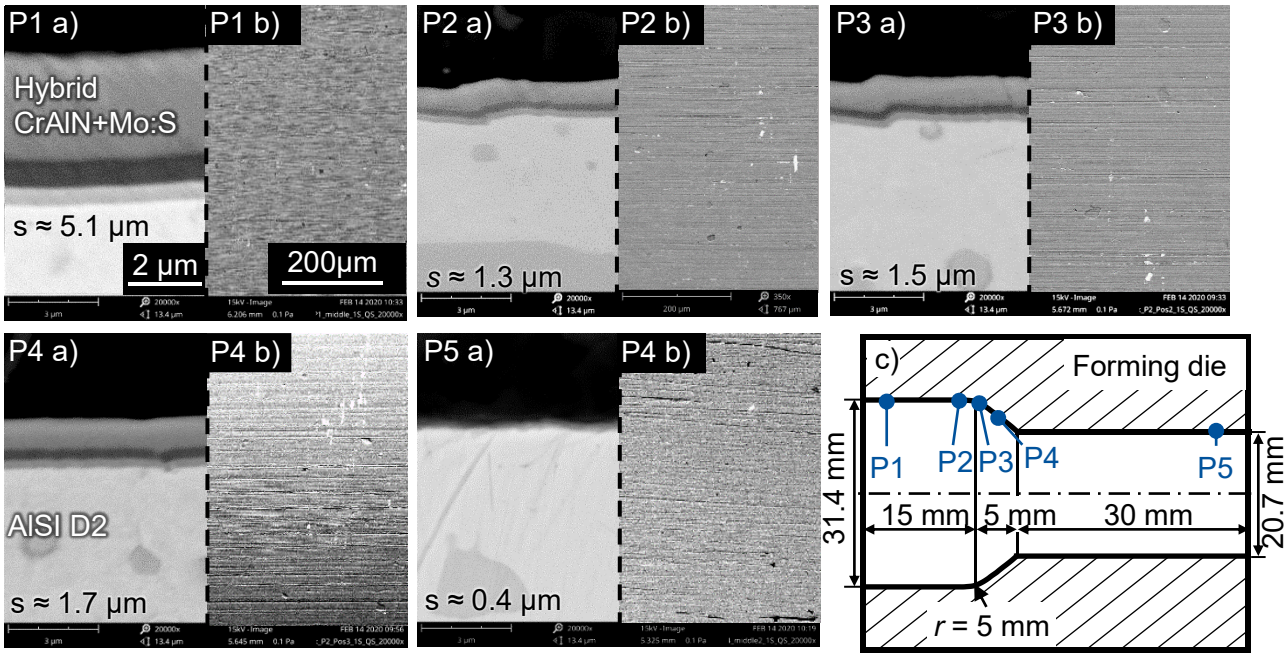

Fig. 24: SEM images of the coated die, tested with reference workpieces, in cross section (a), in top view (b), along the extrusion direction from P1 to P5 (c)

In order to analyze the coating adhesion to the substrate and wear of the applied self-lubricating tool coating hybrid CrAlN+Mo:S, pieces were cut out along the die and metallographically prepared in cross section, Fig. 24 (a). In addition, SEM images of the surface were taken at a higher magnification, Fig. 24 (b). The respective measuring positions from the inlet area over the reduction shoulder to the outlet area are shown in Fig. 24 (c). The cross sections show excellent adhesion of the coating to the substrate. There was no delamination or crack formation. Furthermore, the distribution of the coating thickness as a function of the hole depth could be seen. In comparison to the preliminary investigations using the experimental die model, the coating thickness distribution are comparable. The inlet area is an exception with a higher coating thickness of s ≈ 5 µm. On the basis of the SEM images in top view, it can be seen that no adhesive and abrasive wear can be detected in the inlet and outlet areas after three dry forming tests. Minor adhesive cold weldings of the workpiece material are visible exclusively along the reduction shoulder. These are not spalling, which was verified by means of EDS. Analyses of the coated dies, which were tested with the three different workpiece structures, reveal comparable results. However, a slight increase in adhesive wear can be seen with increasing workpiece roughness.

For further analysis of the influence of die wear, field trials with ten strokes each were carried out with new single-shouldered dies on which the same coating system hybrid CrAlN+Mo:S was deposited. The punch force curves of a ceramic-mix peened workpieces are given as an example in Fig. 25. Here, the increase of the punch force over the consecutive stroke is clearly visible. This illustrates that the friction in the process is increased by a consecutive pressing and thus the punch force increases. Over the course of ten strokes, the roughness of the workpiece surface increases continuously, in particular of the corundum-peened workpieces. The increase in surface roughness takes place primarily in the upset shaft area of the workpiece and not in the reduced area of the workpiece. Thus, even before the analysis of the dies, it can be assumed that the greatest wear of the dies occurs in the shaft area and not in the area of the reduction shoulder. The wear analyses led to clear statements regarding die wear in dry one-shouldered full forward impact extrusion, which also correspond to the observations of the force measurements and wear analyses. It was found that the greatest wear occurs at the shaft die and generally in the shaft area. Within this area, however, less abrasive

wear occurred, but rather adhesive wear. This adhesive wear led to a deterioration of the friction conditions and thus to higher punch forces and to a deterioration of the surface quality of the formed workpieces.

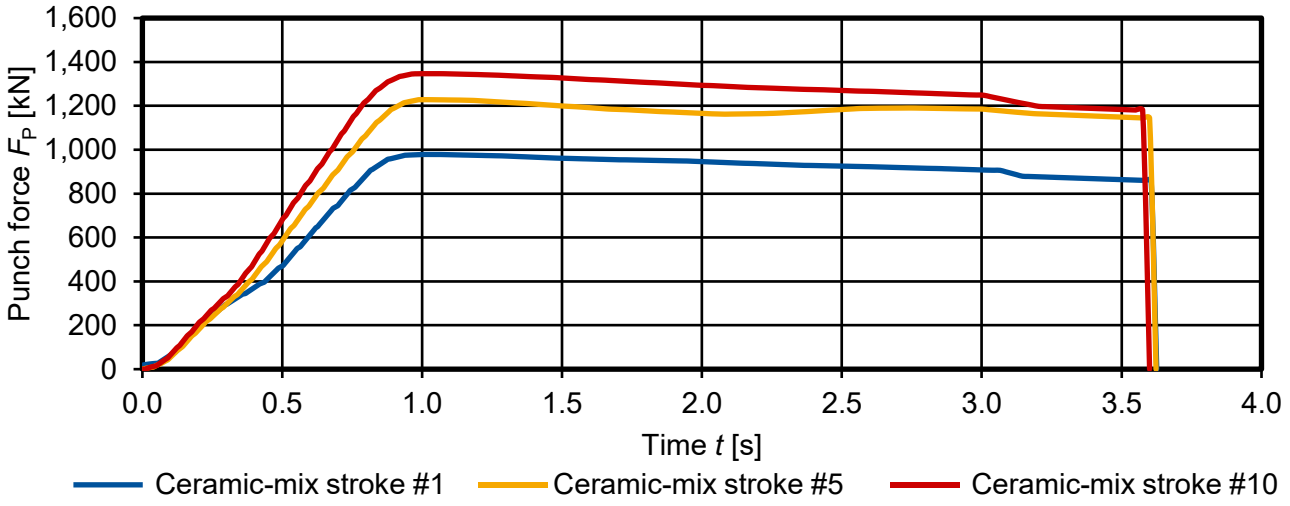

Fig. 25: Force curves of coated die and ceramic-mix-peened workpieces as a function of the number of strokes

In addition to the conspicuousness of the adhesive wear, the area of reduction and in particular the coating was analyzed in more detail. For this purpose, the forming die was analyzed with the help of a scanning electron microscope. No wear could be detected in this area. The coating was largely intact and showed no flaking or reduction in the coating thickness. After all tests, the coating thickness was in a comparable range to the coating thickness of the analogous tools used to prove the coating of the reduction area of the die. This proved that the coating would continue to reduce friction in the process on the one hand and that a reduction of abrasive wear was achieved on the other hand.

6.2 Tribological behavior in two-shouldered field trials

Fig. 26 shows the punch force over time of coated and uncoated two-shouldered dies as a function of workpiece structure of the first stroke without the use of lubricants. To determine the influence of the workpiece structure on the required punch force and the resulting wear, a separate die was tested for each workpiece structure. Accordingly, a total of eight dies, four coated and four uncoated, were tested. Only the results after one stroke are shown here, since the workpieces formed with uncoated dies could not be ejected. Therefore, no further forming tests with uncoated dies were possible. The maximum ejection force of forming press used is F_{eject} = 600 N. Due to very pronounced adhesive wear between uncoated die and workpiece, the ejection force was not sufficient to remove the workpiece out of the die. For this reason, the forming dies had to be disassembled and then mounted rotated by 180°, so that the workpiece could be ejected with the higher available punch force of the press.

During the field trials with all coated dies, the workpieces could be ejected without any problems. Since the workpieces tested by the coated dies could be ejected well, two additional forming tests were carried out for each workpiece structure. Hereby only a slight increase of the maximum force of ΔF_p, Stroke 1 to Stroke 3 ≈ 5 % could be recorded. Basically, Fig. 26 reveals that the necessary punch force of the forming tests with coated dies is lower for each workpiece structure compared to the uncoated dies at the first and second shoulder, respectively. The lowest maximum punch force was achieved with the reference workpiece with F_p = 1.200 kN. Compared to the uncoated tool, the force was reduced by ΔF_p ≈ 15 %. The forces for the peened workpieces with steel beads and the ceramic mix are comparable to those of the reference workpiece. The workpiece structure, which was achieved by means of corundum peening medium, is not appropriate for two-shouldered forming, as these cause the highest forces in coated and uncoated dies. In order to be able to compare the results, which were obtained under dry, unlubricated boundary conditions with the necessary forming forces, with the industrial state of the art, further tests were carried out with phosphated workpieces. The maximum punshing force amounts to F_p = 1,150 kN, regardless of whether coated or uncoated and independent of the workpiece structuring were tested. Since after ten strokes of each workpiece structure no difference in the force curves can be seen when using coated and uncoated dies, it is not shown here. The comparison of the two-shouldered field trials with phosphated and not phosphated workpieces clearly demonstrates that almost the same maximum forming force can be achieved with the self-lubricating PVD coating developed for dry solid forming as with phosphated workpieces.

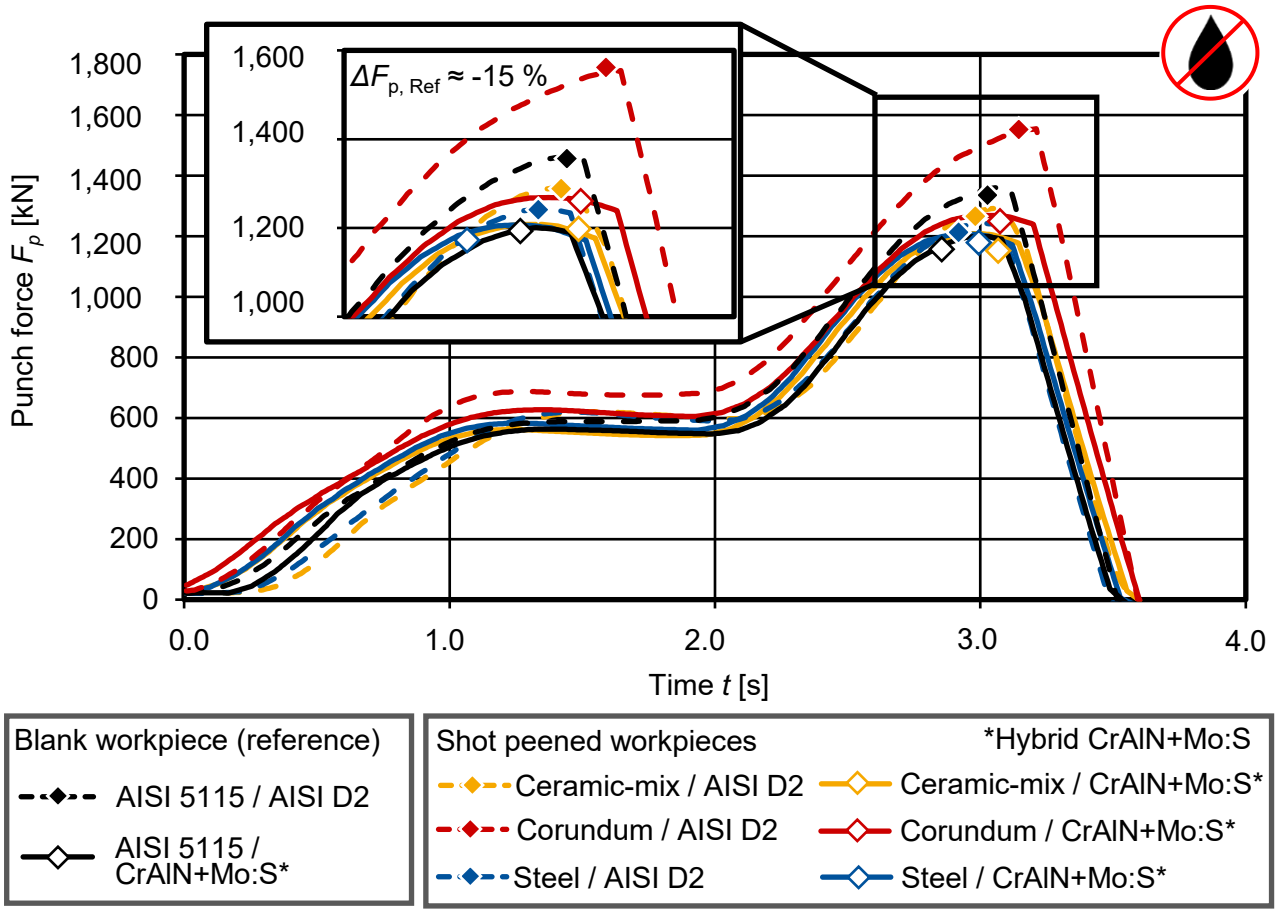

Fig. 26: Force curves of dry two-shouldered full forward impact extrusion as a function of the workpiece structure and the tool coating

Photographs were taken to analyze the wear, Fig. 27. These pictures of the coated dies show the tool condition after three unlubricated strokes respectively, those of the uncoated dies after one stroke.

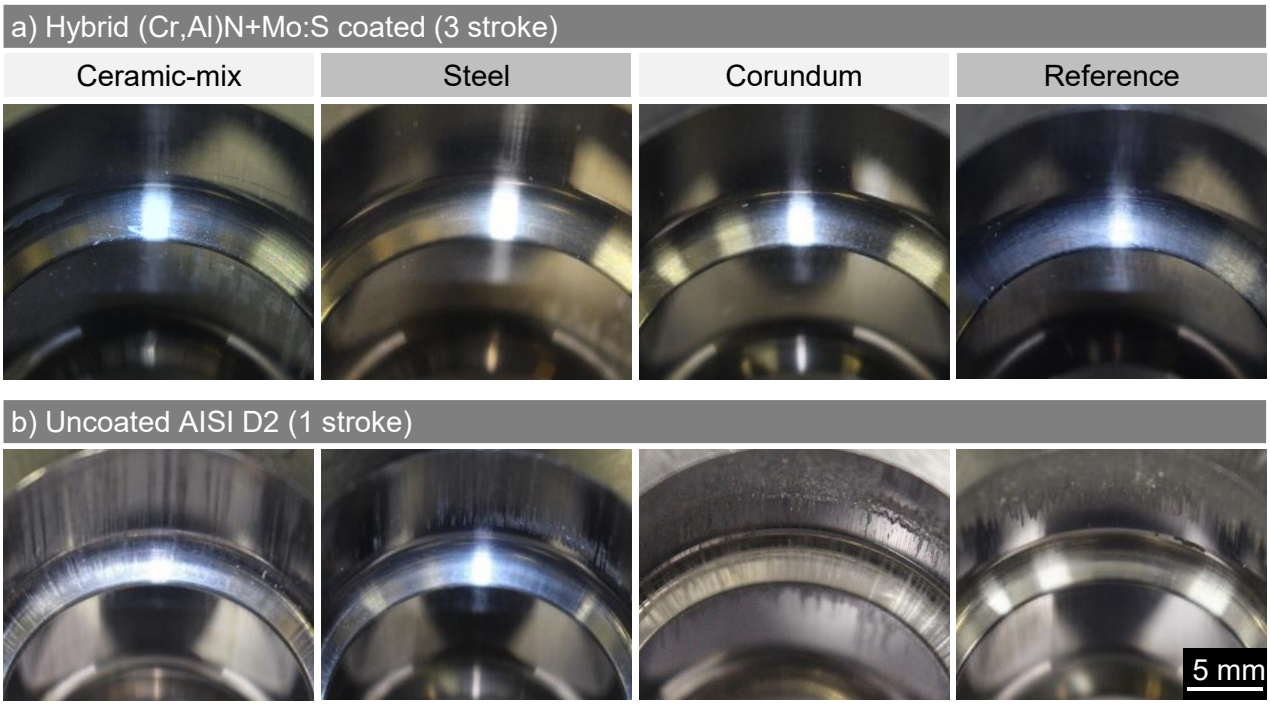

Fig. 27: Camera images of the coated two-shoulder dies after three strokes and the uncoated dies after one stroke under dry boundary conditions depending on the workpiece structure

The coated dies show almost no wear, whereas the uncoated dies show significant wear. The uncoated dies used to form the reference workpiece and the corundum-peened workpiece exhibit significant adhesive wear.

The dies structured with ceramic mix and steel beads led to superimposed adhesive and abrasive wear. Based on the wear of the uncoated dies, it can be seen that the workpieces could not be ejected conventionally.

6.3 Numerical investigation of dry impact extrusion

Numerical FE process simulations of the one-shouldered full forward impact extrusion process were carried out to examine the occurring stresses and the dissipating energy in the form of heat and published in [59]. In initial analyses it became clear that conventional friction models do not have the potential to represent the dry impact extrusion process. On the one hand, there are differences in the amount of punch force and on the other hand, there are discrepancies in the punch force curve. For this reason, after intensive research of existing friction models, a new friction model, which integrates the levelling factor, was developed. With the help of this friction model it was possible to reproduce the dry extrusion process exactly. Exemplarily, the punch force curve for the experimental as well as for the numerical process control is shown in Fig. 28.

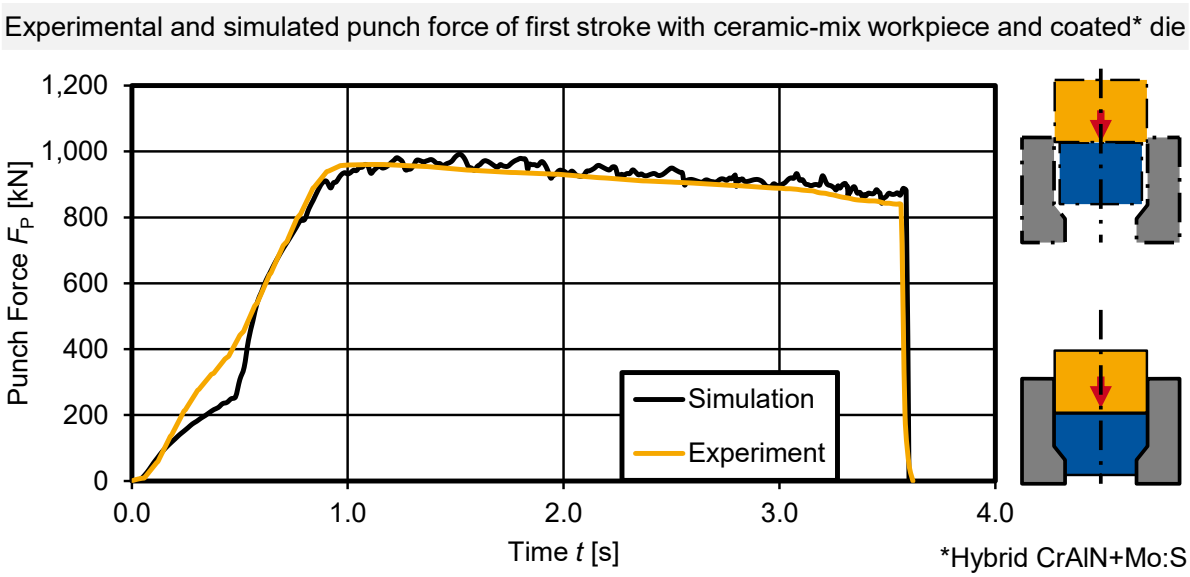

Fig. 28: Validation of the friction model based on the numerical and experimental force curve using the workpiece material AISI 5115

Slight differences in the force increase can be seen at the beginning. These are due to the elasticity of the real tool. The numerical FE process simulation was also modelled with elastic tools, which allowed a clear approximation of the force curves. In the further course the maximum force is achieved with high accuracy. After reaching the force maximum, the necessary force decreases continuously according to the smaller contact area of the component. This process is also the same with high accuracy. In addition, the model was validated on the basis of the simulated final geometry, which was also completely consistent. Thus it was shown that with the help of the new friction model a good agreement of the illustration of the dry impact extrusion process is possible.

The wear model according to Archard was used to determine the abrasive wear numerically. The Archard wear model describes the volume loss of a component. This volume loss depends on the hardness of the component, on the contact normal stress applied to the component and finally on the distance covered by the counterpart, which also applies the contact normal stress. This wear model was used in hot forging, as there a hardness reduction occurs due to the heat, but the model has also been used for cold bulk metal forming. The results of the numerical FE process simulation show in particular the development of wear in the area of reduction, see Fig. 29. Particularly, the reason for this is the high contact normal stresses as well as further increasing relative speeds in this area, as well as the greater distance covered due to the increase in surface area of the workpieces during impact extrusion. The numerical results confirm the assumptions that the highest wear occurs in the area of the highest load. In comparison of the wear simulation with the wear investigations after the dry field trials after three strokes, it can be seen that along the reduction shoulder mostly adhesive and only little abrasive wear occurs.

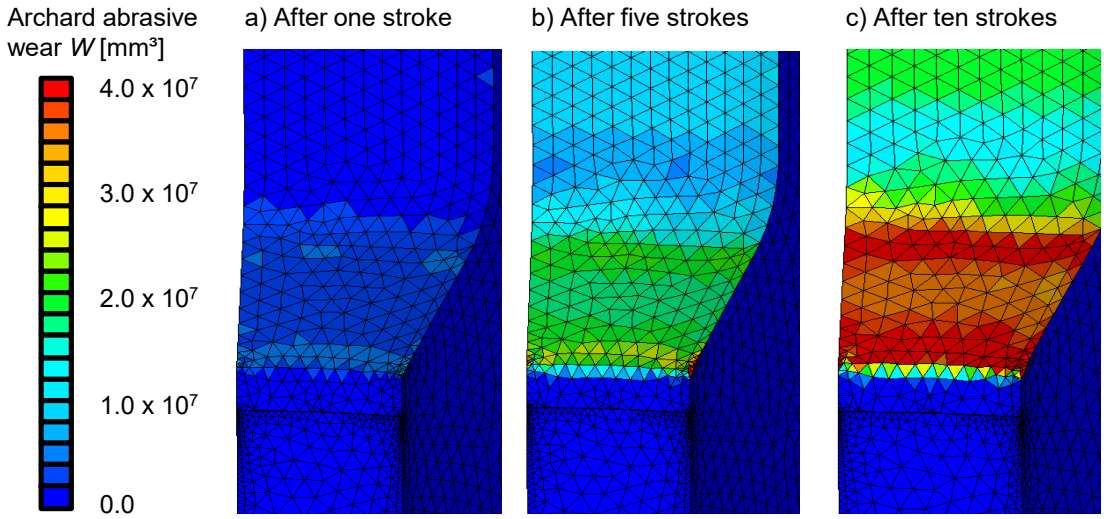

Fig. 29: Archard wear as a function of the impact extrusion process

With the help of levelling it was possible to explain the potential for reducing friction during the first stroke due to the surface texture. Furthermore, it was shown that friction could be reduced depending on the tool coating used. The interactions could be successfully modelled using a friction model, which shows both the coating using the coefficient of friction and the levelling as a factor. Within the experiments, mainly adhesive wear occurred. In the process, matrices worn out faster, in which textured semi-finished products were used. The cause is the locally higher contact normal stresses which lead to cold welding. Due to the roughness peaks, high contact normal stresses occur locally on a microscopic scale, which do not occur with the smooth reference surface. In addition, there is no lubricant separating the two active partners. Adhesive wear therefore occurs in this area.

7 Conclusion

In the scope of the cooperation research project of the IOT and the WZL, dry cold bulk metal forming by full forward impact extrusion of steel workpieces of AISI 5115 without lubricating conversion layers was achieved for the first time on an industrial scale. To achieve this objective, a tool-sided approach of applying self-lubricating, wear-resistant PVD tool coatings and a workpiece-sided approach of surface structuring of the workpieces by means of shot peening were pursued. First the influence of the surface structure on the levelling behavior during plastic forming was analyzed. On the coating sided approach, a parameter window for the deposition of the coating system CrAlN+Mo:S and CrAlN+W:S was determined during process development. In tribological model tests, the friction reducing properties as well as the wear resistance of the developed self-lubricating PVD coatings was proven. To analyze the interaction between different surface structures and self-lubricating coatings, the WZL has constructed the PoC tribometer, which is an open tribological system. Furthermore, the WZL has added a temperature device to the PoC tribometer to account for the influence of the dissipation heat occurring during cold bulk metal forming. For the tool-sided approach, the IOT provided pins with adjusted coating properties to investigate the influence of the workpiece-sided approach of the workpiece structures of the WZL on the dry tribological behavior. Here, a significant reduction in friction and wear was shown. Since a significant reduction in friction and wear was achieved in tribological model tests as a result of the combination of the tool-sided and the workpiece-sided approaches, the findings were used for the first achievement of a dry industrial full forward impact extrusion process. Therefore, the real dies were deposited using the modified industrial coating unit CC800/9 at the IOT for subsequent industrial field trials conducted at the WZL. Initially, the effectiveness of both approaches was demonstrated in lubricated field trials with the environmentally friendly liquid lubricant Fuchs WISURA 3368. The first dry bulk metal forming of steel by full forward impact extrusion of non-phosphated workpieces was achieved. A reduction of the punch force by ΔF_p = -40 % was achieved with the combination of ceramic-mix-peened workpieces and self-lubricating tool coating compared to the field trials with uncoated tool and unstructured workpiece surface.

Subsequently, dry one-shouldered field trials were conducted for the first time. When considering the punch force of the first stroke, the lowest forces could be achieved with the combination of self-lubricating tool coating and corundum-peened workpieces. Considering the punch force after three consecutive strokes, the influence of the occurring tool wear in dependence of the different surface structures becomes apparent. As

wear increases significantly with increasing workpiece roughness, the lowest averaged punch force over three strokes was achieved with coated tools and blank workpieces. Wear investigations of the coated dies after three strokes tested under dry boundary conditions with various workpiece structures reveal that less to no significant signs of wear can be detected. However, in the case of coated dies, it can also be seen that wear increases as the workpiece structure becomes rougher. Furthermore, the self-lubricating coating CrAlN+Mo:S deposited on the real forming dies exhibits a consistently excellent adhesion to the tool substrate after the dry field trials. This shows that PVD coatings are suitable for the application on highly loaded bulk metal forming dies coatings with complex geometries. Additionally, FEM (finite element method) simulations were used to successfully simulate the friction in dry forming process.

Subsequently, two-shouldered field trials were conducted for the first time, which are associated with an enhanced load collective compared to the one-shouldered field trials. These field trials demonstrate that all workpiece variants tested with uncoated forming dies could not be ejected after only one stroke, which is why only one stroke was performed with uncoated dies. By means of the self-lubricating coating it could be shown that all workpieces could be ejected even after three strokes. Furthermore, the lowest necessary punch force was achieved with the coated die. However, the influence of the workpiece structuring on the punch force in two-shouldered field trials is less than in one-shoulder field trials due to the changed load collective. Furthermore, the self-lubricating tool coating significantly reduces wear. The coated dies exhibit almost no wear after three strokes, whereas the uncoated dies show significant adhesive and partially abrasive wear after a single stroke. When comparing two-shouldered field trials with phosphated workpieces with the field trials carried out under dry boundary conditions, the maximum necessary punch force is only slightly higher with approximately $\Delta F_p = +5$ %. In summary, it can be stated that the tool-sided approach of application of self-lubricating, wear resistant tool coatings and the workpiece-sided approach of workpiece structuring pursued in this research project are appropriate for the achievement of dry full forward impact extrusion of steel.

8 Outlook

Based on the promising industrial dry field trials, further forming tests with higher lot sizes are planned to investigate the wear resistance as a function of higher quantities of workpieces. For a first application in industry, the implementation of a forming process on an industrial scale with high lot sizes by means of environmentally friendly liquid lubricants that are not harmful to health is conceivable. In this way, the conventional lubrication currently established in the state of the art by workpiece phosphating and the use of further solid and liquid lubricants as well as various additives, which are associated with ecological and economic disadvantages as well as health-dangerous aspects, can be substituted. Furthermore, the objective is the complete substitution of all lubricants while maintaining process stability and product quality. In particular, the tool-side approach of applying PVD tool coatings reveals promising potential for use in the environmentally friendly mass production of workpieces formed by cold bulk metal forming. Moreover, the findings can be transferred to other workpiece materials, such as aluminium alloys. A transfer to other forming processes such as sheet metal forming is also conceivable.

Acknowledgements

The research was funded by the German Research Foundation (Deutsche Forschungsgemeinschaft DFG, BO 1979/44-2; KL 500/141-2) within the priority program „Dry metal forming – sustainable production through dry processing in metal forming (SPP 1676).

References

[1] F. Klocke: Manufacturing Processes 4, Springer Berlin Heidelberg, Berlin, Heidelberg (2013).

[2] K. Lange, M. Kammerer, K. Pöhlandt, J. Schöck: Fließpressen: Wirtschaftliche Fertigung metallischer Präzisionswerkstücke, Springer, Berlin (2008).

[3] DIN: Manufacturing processes forming - Classification; Subdivision, terms and definitions, alphabetical index.

[4] Soyarslan C., A. Tekkaya: Prevention of internal Cracks in Forward Extrusion by Means of Counter Pressure:. A Numerical Treatise. Steel Research International 80 (2009) 4–12.

[5] E. Doege, B.-A. Behrens: Handbuch Umformtechnik: Grundlagen, Technologien, Maschinen, 2nd ed., Springer-Verlag, s.l. (2010).

[6] C. Coulomb: Theorie des machines simples, en ayant Â´egard au frottement de leurs parties et a la roideur des cordages: Memoires de mathematique et de physique de L'Académie des Sciences (1785).

[7] F.P. Bowden, D. Tabor, E.H. Freitag: Reibung und Schmierung fester Körper, Springer Berlin Heidelberg, Berlin, Heidelberg (1959).

[8] D.-K. Leu: A simple dry friction model for metal forming process. Journal of Materials Processing Technology 209 5 (2009) 2361–2368.

[9] M. Shaw: The role of friction in deformation processing. Wear 6 2 (1963) 140–158.

[10] N. Bay, M. Eriksen, X. Tan, O. Wibom: An empirical model for friction in cold forging. Proceedings of Euromech 435 (2002) 105–124.

[11] A. Bouguecha, T. Hadifi, J. Mielke, B.-A. Behrens: Erhöhung der Berechnungsgenauigkeit bei der numerischen Abbildung von Warmmassivumformprozessen durch verbesserte Reibmodellierung. Mat.-wiss. u. Werkstofftech. 43 10 (2012) 839–850.

[12] J. Filzek: Umformen, Schneiden, Verbinden im Leichtbau: Machbarkeit - Produktivität - Qualität; Tagungsband des 33. EFB-Kolloquiums Blechverarbeitung, Fellbach, 16.04-17.04 (2013).

[13] N. Bay, A. Azushima, P. Groche, I. Ishibashi, M. Merklein, M. Morishita, T. Nakamura, S. Schmid, M. Yoshida: Environmentally benign tribo-systems for metal forming. CIRP Annals 59 2 (2010) 760–780.

[14] P.-M. Mattfeld: Tribologie der zinkphosphatfreien Kaltmassivumformung. Zugl.: Aachen, Techn. Hochsch., Diss., 2013, 1st ed., Apprimus-Verl., Aachen (2014).

[15] D.M. Mattox: Handbook of physical vapor deposition (PVD) processing, 2nd ed., William Andrew, Amsterdam (2010).

[16] F. Vollertsen, F. Schmidt: Dry metal forming: Definition, Chances and Challenges. Int. J. Precision Engineering and Manufacturing - Green Technology 1/1 (2014) 59–62.

[17] H. Czichos, K.-H. Habig: Tribologie-Handbuch: Tribometrie, Tribomaterialien, Tribotechnik, 4th ed., Springer Vieweg, Wiesbaden (2015).

[18] M. Murakawa, S. Takeuchi: Evaluation of tribological properties of DLC films used in sheet forming of aluminum sheet. Surface and Coatings Technology 163-164 (2003) 561–565.

[19] K. Osakada, R. Matsumoto: Fundamental Study of Dry Metal Forming with Coated Tools. CIRP Annals 49 1 (2000) 161–164.

[20] J.-F. Yang, B. Parakash, J. Hardell, Q.-F. Fang: Tribological properties of transition metal di-chalcogenide based lubricant coatings. Front. Mater. Sci. 6 2 (2012) 116–127.

[21] L. Lind, E. Adoberg, L. Aarik, P. Kulu, R. Veinthal, A.A. Aal: Tribological properties of PVD coatings with lubricating films. Estonian J. Eng. 18 3 (2012) 193.

[22] K. Bobzin, T. Brögelmann, N. C. Kruppe, M. Arghavani, S. Bastürk, F. Klocke, P. Mattfeld, D. Trauth, R. Hild: Dry Met. Forming OAJ FMT 2 (2016) 72–77.

[23] K. Bobzin, T. Brögelmann, N.C. Kruppe, D.C. Hoffmann, F. Klocke, P. Mattfeld, D. Trauth, R. Hild: Tribological studies on self-lubricating (Cr,Al)N+Mo:S coatings at elevated temperature. Surface and Coatings Technology 353 (2018) 282–291.

[24] K. Bobzin, T. Brögelmann, N.C. Kruppe, M. Arghavani, D.C. Hoffmann, F. Klocke, P. Mattfeld, D. Trauth, R. Hild: Mechanical and tribological characterization of self-lubricating ($Cr_{1-x}Al_x$)N coatings for deposition on complex-shaped forging tools. Dry Met. Forming OAJ FMT 3 (2017) 81–89.

[25] K. Bobzin, T. Brögelmann, N.C. Kruppe, M. Arghavani, D.C. Hoffmann, F. Klocke, P. Mattfeld, D. Trauth, R. Hild: Influence of the bias voltage on the mechanical and tribological behavior of self-lubricating hybrid dcMS/HPPMS (Cr,Al)N coatings. Proceedings of the 13th International Conference THe „A“ coatings in Manufacturing Engineering, Thessaloniki, Greece, October 5th - 6th (2017) (2017) 149–158.

[26] T. Spalvins: A review of recent advances in solid film lubrication. Journal of Vacuum Science & Technology A: Vacuum, Surfaces, and Films 5 2 (1987) 212–219.

[27] A. Aubert, J.P. Nabot, J. Ernoult, P. Renaux: Preparation and properties of MoS_x films grown by d.c. magnetron sputtering. Surface and Coatings Technology 41 1 (1990) 127–134.

[28] B. Tlili, N. Mustapha, C. Nouveau, Y. Benlatreche, G. Guillemot, M. Lambertin: Correlation between thermal properties and aluminum fractions in CrAlN layers deposited by PVD technique. Vacuum 84 9 (2010) 1067–1074.

[29] K. Bobzin, T. Brögelmann, N.C. Kruppe, M. Arghavani: Investigations on Mechanical and Tribological Behavior of dcMS/HPPMS CrN and (Cr,Al)N Hard Coatings Using Nanoscratch Technique. Adv. Eng. Mater. 19 6 (2017) 1600632.

[30] J. Čapek, M. Hála, O. Zabeida, J.E. Klemberg-Sapieha, L. Martinu: Deposition rate enhancement in HiPIMS without compromising the ionized fraction of the deposition flux. J. Phys. D: Appl. Phys. 46 20 (2013) 205205.

[31] K. Bobzin, N. Bagcivan, P. Immich, S. Bolz, R. Cremer, T. Leyendecker: Mechanical properties and oxidation behaviour of (Al,Cr)N and (Al,Cr,Si)N coatings for cutting tools deposited by HPPMS. Thin Solid Films 517 3 (2008) 1251–1256.

[32] R. Bandorf, V. Sittinger, G. Bräuer: High Power Impulse Magnetron Sputtering – HIPIMS, in: S. Hashmi (Ed.), Comprehensive Materials Processing, Elsevier, Oxford, 2014, pp. 75–99.

[33] N. Bagcivan, K. Bobzin, S. Theiß: ($Cr_{1-x}Al_x$)N: A comparison of direct current, middle frequency pulsed and high power pulsed magnetron sputtering for injection molding components. Thin Solid Films 528 (2013) 180–186.

[34] H. Murrenhoff: Umweltverträgliche Tribosysteme: Die Vision einer umweltfreundlichen Werkzeugmaschine, Springer-Verlag Berlin Heidelberg, Berlin, Heidelberg (2010).

[35] M. Köhler: Beitrag zur zinkphosphatschichtfreien Kaltmassivumformung durch tribologisch vorteilhafte Halbzeugoberflächen. Zugl.: Darmstadt, Techn. Univ., Diss., 2009, Shaker, Aachen (2010).

[36] J. Stahlmann, E.R. Nicodemus, S.C. Sharma, P. Groche: Surface roughness evolution in FEA simulations of bulk metal forming process. Wear 288 (2012) 78–87.

[37] J. Hol: Multi-scale friction medeling for sheet metal forming, Enschede (2013).

[38] J. Hol, V.T. Meinders, H.J.M. Geijselaers, A.H. van den Boogaard: Multi-scale friction modeling for sheet metal forming: The mixed lubrication regime. Tribology International 85 (2015) 10–25.

[39] K.-H. Grote, E.K. Antonsson: Springer handbook of mechanical engineering, Springer-Verlag, Berlin Heidelberg (2009).

[40] W.C. Oliver, G.M. Pharr: An improved technique for determining hardness and elastic modulus using load and displacement sensing indentation experiments. J. Mater. Res. 7 06 (1992) 1564–1583.

[41] D. Trauth, R. Hild, P. Mattfeld, S. Bastürk, T. Brögelmann, K. Bobzin, F. Klocke: Advances in dry metal forming of low alloyed steels for cold forging using a (Cr,Al)N tool coating and surface structures on workpieces. Proceedings of the 12th International Conference THe „A“ coatings in Manufacturing Engineering, Hannover, Germany, March 31th - April 1st (2016).

[42] R. Hild, R. Mannens, D. Trauth, P. Mattfeld, T. Bergs, D.C. Hoffmann, N.C. Kruppe, T. Brögelmann, K. Bobzin: Investigation of friction and adhesion behavior of textured workpieces and coated tools udner try tribolocigal contact. TMS 2019 148th Annual Meeting & Exhibition Supplemental Proceedings, Springer International Publishing, Cham (2019).

[43] A.R. Lansdown: Molybdenum disulphide lubrication, 1st ed., Elsevier, Amsterdam (1999).

[44] M.A. Baker, R. Gilmore, C. Lenardi, W. Gissler: XPS investigation of preferential sputtering of S from MoS_2 and determination of MoS_x stoichiometry from Mo and S peak positions. Applied Surface Science 150 1-4 (1999) 255–262.

[45] J. Moser, F. Lévy, F. Bussy: Composition and growth mode of MoS_x sputtered films. Journal of Vacuum Science & Technology A: Vacuum, Surfaces, and Films 12 2 (1994) 494–500.

[46] B. Chapman: Glow discharge processes, John Wiley & Sons, Incorporated, Chichester (1980).

[47] K. Bobzin, T. Brögelmann, N.C. Kruppe, S. Basturk, F. Klocke, P. Mattfeld, D. Trauth, R. Hild: Synthesis, characterization, and tribological evaluation of HPPMS $(Cr_{1-x}Al_x)N + MoS_y$ coatings. Surface and Coatings Technology 308 (2016) 383–393.

[48] K. Bobzin, T. Brögelmann, N.C. Kruppe, M. Arghavani, S. Bastürk, F. Klocke, P. Mattfeld, D. Trauth, R. Hild: HPPMS $(CR_{1-x}Al_x)+WS_y$ Coatings for the Application in Dry Cold Forging of Steel: Synthesis and Raman Characterization. Dry Met. Forming OAJ FMT 2 (2016) 72–77.

[49] K. Bobzin, T. Brögelmann, N.C. Kruppe, S. Bastürk, F. Klocke, P. Mattfeld, D. Trauth: Tribological Behavior of $(Cr_{1-x}Al_x)N/WS_y$ PVD Tool Coatings for the Application in Dry Cold Forging of Steel. Dry Met. Forming OAJ FMT 1 (2015) 152–158.

[50] K. Bobzin, T. Brögelmann, R.H. Brugnara, N.C. Kruppe, S. Bastürk, F. Klocke, P. Mattfeld, R. Hild, D. Trauth: Influence of the Chemical Composition on the Properties of HPPMS $(Cr_{1-x},Al_x)WS_y$ Coatings for the Application in Dry Cold Forging Processes. Proceedings of the 12th International Conference THe „A“ coatings in Manufacturing Engineering, Hannover, Germany, March 31st - 1st (2016) (2016) 161–168.

[51] Bobzin K., T. Brögelmann, Kruppe N.C., Hoffmann D.C., Klocke F., T. Bergs, Trauth D., Mannens R., Hild R.: In Proceedings of the 59th Tribologie-Fachtagung: Tribologie selbstschmierender PVD-Schichten für die trockene Kaltmassivumformung, 47th ed., Göttingen (2018).

[52] L. Bellot-Gurlet, D. Neff, S. Réguer, J. Monnier, M. Saheb, P. Dillmann: Raman Studies of Corrosion Layers Formed on Archaeological Irons in Various Media. JNanoR 8 (2009) 147–156.

[53] D. Chicot, J. Mendoza, A. Zaoui, G. Louis, V. Lepingle, F. Roudet, J. Lesage: Mechanical properties of magnetite (Fe_3O_4), hematite (α-Fe_2O_3) and goethite (α-FeO·OH) by instrumented indentation and molecular dynamics analysis. Materials Chemistry and Physics 129 3 (2011) 862–870.

[54] K. Mistry, A. Morina, A. Neville: Single cam tribometer for evaluating tribological parameters and tribochemistry of DLC coated valve train follower. Tribology - Materials, Surfaces & Interfaces 6 1 (2013) 31–37.

[55] K. Bobzin, T. Brögelmann, N.C. Kruppe, T. Bergs, D. Trauth, R. Hild, R. Mannens, D.C. Hoffmann: Self-Lubricating Physical Vapor Deposition Coatings for Dry Cold Massive Forming. steel research int. 2 (2019) 1900475.

[56] F. Klocke, R. Hild, D. Trauth, K. Bobzin, T. Brögelmann, N.C. Kruppe, D.C. Hoffmann: Einfluss von Oberflächenstrukturierungen auf die Stempelkraft beim Vollvorwärtsfließpressen von 16MnCr5. Dry Met. Forming OAJ FMT 4 (2018) 25–30.

[57] J.W. Raedt, F. Klocke: Grundlagen für das schmiermittelreduzierte Tribosystem bei der Kaltumformung des Einsatzstahles 16 MnCr 5: Fakultät für Maschinenwesen.

[58] R. Hild, T. Bergs, P. Mattfeld, D. Trauth, F. Klocke, D.C. Hoffmann, N.C. Kruppe, T. Brögelmann, K. Bobzin: Analysis of wear phenomena during forward extrusion under dry friction conditions. Wear 426-427 (2019) 1362–1370.

[59] R. Hild, A. Feuerhack, D. Trauth, M. Arghavani, N. Kruppe, T. Brögelmann, K. Bobzin, F. Klocke: Suitablility of friction lows to simulate the infuence of surface textures on the process force in cold forging. Proceedings of the 13th International Conference THe „A“ coatings in Manufacturing Engineering, Thessaloniki, Greece, October 5th - 6th (2017) (2017) 103–111.